DESY-05-094
JLAB-THY-05-375
hep-ph/0506171

Exclusive channels in semi-inclusive production of pions and kaons

M. Diehl, W. Kugler

Deutsches Elektronen-Synchroton DESY, 22603 Hamburg, Germany

A. Schäfer

Institut für Theoretische Physik, Universität Regensburg, 93040 Regensburg, Germany

C. Weiss

Theory Group, Jefferson Lab, Newport News, VA 23606, U.S.A.

Abstract

We investigate the role of exclusive channels in semi-inclusive electroproduction of pions and kaons. Using the QCD factorization theorem for hard exclusive processes we evaluate the cross sections for exclusive pseudoscalar and vector meson production in terms of generalized parton distributions and meson distribution amplitudes. We investigate the uncertainties arising from the modeling of the nonperturbative input quantities. Combining these results with available experimental data, we compare the cross sections for exclusive channels to that obtained from quark fragmentation in semi-inclusive deep inelastic scattering. We find that ρ^0 production is the only exclusive channel with significant contributions to semi-inclusive pion production at large z and moderate Q^2. The corresponding contribution to kaon production from the decay of exclusively produced ϕ and K^* is rather small.

Contents

1 Introduction

Electroproduction processes in the Bjorken regime probe the partonic structure of the nucleon. Inclusive deep inelastic scattering (DIS) provides extensive information about the sum of quark and antiquark distributions in the nucleon, and allows one to determine the gluon distribution from the observed scaling violations. More detailed information can be obtained from scattering experiments in which one or more hadrons are observed in the final state. There are two basic classes of such experiments. The first one is semi-inclusive deep inelastic scattering, in which one observes a single hadron, carrying a fraction z of the photon energy in the target rest frame, in a final state of large average multiplicity. A QCD factorization theorem states that the semi-inclusive cross section in the Bjorken limit can be expressed in terms of distribution functions for quarks, antiquarks and gluons in the target and of the corresponding fragmentation functions into the observed hadron. This allows one to tag the active parton via its fragmentation properties and has recently been used for a flavor decomposition of polarized quark and antiquark distributions in the semi-inclusive production of pions and kaons [1]. In addition, measurements of azimuthal asymmetries in semi-inclusive pion and kaon production, such as the Collins and Sivers asymmetries for a transversely polarized target [2], provide interesting information about the distribution of the spin and transverse momentum carried by quarks and antiquarks in the nucleon.

The second class are exclusive scattering processes, in which the final state is a recoiling baryon B together with a single meson or a few-meson system carrying nearly the full photon energy in the target rest frame. A QCD factorization theorem states that in the Bjorken limit, and for longitudinal photon polarization, the amplitudes of such processes are calculable in terms of the light-cone distribution amplitude of the produced meson and generalized parton distributions (GPDs) for the $p \to B$ transition. Generalized parton distributions provide a wealth of information on the parton structure of the nucleon, in particular about the spatial distribution of partons in the transverse plane and about quark orbital angular momentum, see e.g. the reviews [3, 4, 5, 6, 7].

The Bjorken limit for semi-inclusive electroproduction implies a large average multiplicity of the produced hadronic system. In practice, however, there can be situations in which individual exclusive channels play an important role. In fixed-target experiments the limited photon energy restricts the phase space for quark fragmentation, in particular at large z, and for relatively low photon virtuality Q^2 the suppression of individual exclusive channels due to the faster drop of the exclusive cross sections with Q^2 may not yet be effective. In particular, phenomenological studies suggest that a large contribution to $\pi^\pm$ production comes from exclusive ρ^0 production, with subsequent decay $\rho^0 \to \pi^+\pi^-$ [8, 9]. Fortunately, the cross sections for exclusive ρ^0 electroproduction has been measured by the HERMES and CLAS experiments, including the cross section ratio for longitudinal and transverse photons [10, 11, 12, 13, 14]. It is natural to ask whether the strange vector mesons ϕ and K^* play an equally important role in semi-inclusive kaon production and whether other exclusive channels may be important, too. A quantitative answer to these questions will help to delineate the limits of the kinematic region where semi-inclusive data can be analyzed using the factorization theorem.

In this paper we investigate the role of exclusive channels in the semi-inclusive production of pions and kaons on the basis of the factorization theorem for hard exclusive processes. Our investigation consists of two parts. Firstly, we evaluate the longitudinal cross section for the exclusive production of pseudoscalar and vector mesons in the leading-twist approximation and at leading order in the strong coupling, focusing on π, K and ρ, ϕ, K^*. We explore uncertainties in the obtained cross sections, in particular those due to the generalized parton distributions, which are still largely unknown and need to be modeled. Such uncertainties will persist if higher-order and higher-twist corrections are included. Seen from a different perspective, they indicate to which extent exclusive meson production

is sensitive to GPDs and thus interesting in its own right. It is known that exclusive meson production cross sections at moderate Q^2 are affected by substantial power corrections. For the production of ρ^0, ϕ and π^+ there is data or preliminary data, which we will use to assess the quantitative validity of our calculated cross sections. Secondly, we evaluate the contribution of these exclusive channels to semi-inclusive production of π and K, and compare them with the results obtained from leading-twist quark fragmentation. For the exclusive meson production cross sections we rely on experimental data where possible, and only use our leading-twist calculation to estimate the *ratio* of cross sections for measured and unmeasured channels.

The paper is organized as follows. In Sects. 2 and 3 we summarize the leading-twist description of exclusive meson production and describe the models for the GPDs used in our investigation. An analysis of pseudoscalar and vector meson production channels is then given in Sects. 4 and 5. In Sect. 6 we briefly discuss the limitations of our leading-order results and compare them with experimental data. The contribution of exclusive channels to semi-inclusive meson production is compared with leading-twist quark fragmentation in Sect. 7, and in Sect. 8 we summarize our main results. Some important technical details are given in two appendices.

2 Exclusive meson production in the leading-twist approximation

Let us consider the exclusive electroproduction process

$$e(k) \; + \; p(p) \;\; \to \;\; e(k') \; + \; M(q') \; + \; B(p'), \tag{1}$$

where M is a meson and B a baryon, and where four-momenta are indicated in parentheses. Throughout this work we assume beam and target to be unpolarized. We write $q = k - k'$, $\Delta = p' - p$, and use the standard kinematic variables

$$t = \Delta^2, \qquad Q^2 = -q^2, \qquad W^2 = (p+q)^2, \qquad x_B = Q^2/(2pq), \qquad y = (pq)/(pk). \tag{2}$$

We respectively write m_p, m_B, m_M for the masses of the proton, the baryon B, and the meson M. With Hand's convention [16] for the virtual photon flux, the electroproduction cross section is given by

$$\frac{d\sigma(ep \to eMB)}{dQ^2\, dx_B\, dt} = \frac{\alpha_{em}}{2\pi} \frac{y^2}{1-\epsilon} \frac{1-x_B}{x_B} \frac{1}{Q^2} \left[\frac{d\sigma_T}{dt} + \epsilon \frac{d\sigma_L}{dt} \right] \tag{3}$$

in terms of the cross sections $d\sigma_T/dt$ and $d\sigma_L/dt$ of the $\gamma^* p \to MB$ subprocess for transverse and longitudinal γ^*, where

$$\epsilon = \frac{1 - y - (y x_B m_p/Q)^2}{1 - y + y^2/2 + (y x_B m_p/Q)^2} \tag{4}$$

is the ratio of longitudinal to transverse photon flux.

In the generalized Bjorken limit of large Q^2 at fixed x_B and fixed t, the process amplitude factorizes into a hard-scattering kernel convoluted with generalized parton distributions for the $p \to B$ transition and with the distribution amplitude of the meson [15]. Example graphs are shown in Fig. 1. In this limit the longitudinal cross section can be written as

$$\frac{d\sigma_L}{dt} = \frac{\alpha_{em}}{Q^6} \frac{x_B^2}{1-x_B} \left\{ (1-\xi^2) |\mathcal{H}|^2 - \left[\frac{2\xi(m_B^2 - m_p^2) + t}{(m_B + m_p)^2} + \xi^2 \right] |\mathcal{E}|^2 - \left[\xi + \frac{m_B - m_p}{m_B + m_p} \right] 2\xi \, \mathrm{Re}\, (\mathcal{E}^* \mathcal{H}) \right\} \tag{5}$$

for vector mesons, and as

$$\frac{d\sigma_L}{dt} = \frac{\alpha_{em}}{Q^6} \frac{x_B^2}{1-x_B} \left\{ (1-\xi^2) |\tilde{\mathcal{H}}|^2 + \frac{(m_B - m_p)^2 - t}{(m_B + m_p)^2} \xi^2 |\tilde{\mathcal{E}}|^2 - \left[\xi + \frac{m_B - m_p}{m_B + m_p} \right] 2\xi \, \mathrm{Re}\, (\tilde{\mathcal{E}}^* \tilde{\mathcal{H}}) \right\} \tag{6}$$

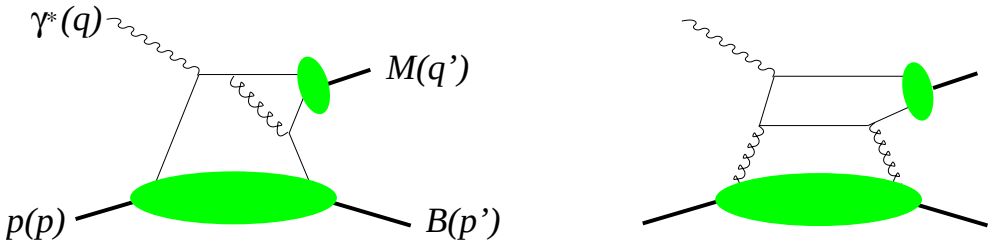

Figure 1: Example graphs for exclusive meson production in the generalized Bjorken limit. The large blob denotes the $p \to B$ transition GPD and the small one the meson distribution amplitude.

for pseudoscalar mesons M. The transverse cross section $d\sigma_T/dt$ is power suppressed by $1/Q^2$ compared with $d\sigma_L/dt$. Here we have in addition used the skewness variable

$$\xi = \frac{(p-p')(q+q')}{(p+p')(q+q')} \approx \frac{x_B}{2-x_B}, \tag{7}$$

where the approximation holds in the generalized Bjorken limit. Note that the prefactor in (5) and (6) can be rewritten as $x_B^2/(1-x_B) = 4\xi^2/(1-\xi^2)$. The quantities $\mathcal{H}$, $\mathcal{E}$ and $\tilde{\mathcal{H}}$, $\tilde{\mathcal{E}}$ are specific for each channel. Throughout this work we will take their leading order approximations in α_s. To be specific, we have

$$\begin{aligned}
\mathcal{H}_{K^{*+}\Lambda}(\xi,t) &= \frac{4\pi\alpha_s}{27} f_{K^*} \left[\int_0^1 dz\, \frac{1}{z(1-z)}\, \phi_{K^{*+}}(z) \int_{-1}^1 dx\, \frac{2H_{p\to\Lambda}(x,\xi,t) + H_{p\to\Lambda}(-x,\xi,t)}{\xi - x - i\varepsilon} \right. \\
&\quad \left. - \int_0^1 dz\, \frac{2z-1}{z(1-z)}\, \phi_{K^{*+}}(z) \int_{-1}^1 dx\, \frac{2H_{p\to\Lambda}(x,\xi,t) - H_{p\to\Lambda}(-x,\xi,t)}{\xi - x - i\varepsilon} \right], \\
\tilde{\mathcal{H}}_{K^{+}\Lambda}(\xi,t) &= \frac{4\pi\alpha_s}{27} f_{K} \left[\int_0^1 dz\, \frac{1}{z(1-z)}\, \phi_{K^{+}}(z) \int_{-1}^1 dx\, \frac{2\tilde{H}_{p\to\Lambda}(x,\xi,t) + \tilde{H}_{p\to\Lambda}(-x,\xi,t)}{\xi - x - i\varepsilon} \right. \\
&\quad \left. - \int_0^1 dz\, \frac{2z-1}{z(1-z)}\, \phi_{K^{+}}(z) \int_{-1}^1 dx\, \frac{2\tilde{H}_{p\to\Lambda}(x,\xi,t) - \tilde{H}_{p\to\Lambda}(-x,\xi,t)}{\xi - x - i\varepsilon} \right]
\end{aligned} \tag{8}$$

for $\gamma^* p \to K^{*+}\Lambda$ and $\gamma^* p \to K^+\Lambda$, respectively, with analogous expressions for $\mathcal{E}_{K^{*+}\Lambda}$ and $\tilde{\mathcal{E}}_{K^+\Lambda}$. The GPDs for the $p \to \Lambda$ transition are defined as

$$\begin{aligned}
&\frac{1}{2}\int \frac{dz^-}{2\pi}\, e^{ixP^+z^-} \langle \Lambda |\, \bar{s}(-\tfrac{1}{2}z)\, \gamma^+ u(\tfrac{1}{2}z)\, |p\rangle \Big|_{z^+=0,\, z_T=0} \\
&\qquad = \frac{1}{2P^+} \left[H_{p\to\Lambda}(x,\xi,t)\, \bar{u}\gamma^+ u + E_{p\to\Lambda}(x,\xi,t)\, \bar{u} \frac{i\sigma^{+\alpha}\Delta_\alpha}{m_\Lambda + m_p} u \right], \\
&\frac{1}{2}\int \frac{dz^-}{2\pi}\, e^{ixP^+z^-} \langle \Lambda |\, \bar{s}(-\tfrac{1}{2}z)\, \gamma^+\gamma_5\, u(\tfrac{1}{2}z)\, |p\rangle \Big|_{z^+=0,\, z_T=0} \\
&\qquad = \frac{1}{2P^+} \left[\tilde{H}_{p\to\Lambda}(x,\xi,t)\, \bar{u}\gamma^+\gamma_5 u + \tilde{E}_{p\to\Lambda}(x,\xi,t)\, \bar{u} \frac{\gamma_5 \Delta^+}{m_\Lambda + m_p} u \right],
\end{aligned} \tag{9}$$

where we use light-cone coordinates $v^\pm = (v^0 \pm v^3)/\sqrt{2}$ and $v_T = (v^1, v^2)$ for a four-vector v and assume light-cone gauge $A^+ = 0$. For brevity we have not displayed the momentum and polarization dependence of the baryon spinors on the right-hand sides. GPDs for other transitions are defined in

Table 1: Combinations of proton GPDs to be used for various channels $\gamma p \to MB$ at the place of $2H_{p\to\Lambda}(x,\xi,t) + H_{p\to\Lambda}(-x,\xi,t)$ or $2\tilde{H}_{p\to\Lambda}(x,\xi,t) + \tilde{H}_{p\to\Lambda}(-x,\xi,t)$ in (8). All distributions are to be evaluated at arguments x, ξ, t, with H^q, $\tilde{H}^q$ and H^g as defined in [6] and $H^{\bar{q}}$, $\tilde{H}^{\bar{q}}$ given above (12).

$\rho^+ n$	$2[H^u - H^d] - [H^{\bar{u}} - H^{\bar{d}}]$
$\rho^0 p$	$\frac{1}{\sqrt{2}}\Big([2H^u + H^d] + [2H^{\bar{u}} + H^{\bar{d}}] + \frac{9}{4}\, x^{-1} H^g \Big)$
ωp	$\frac{1}{\sqrt{2}}\Big([2H^u - H^d] + [2H^{\bar{u}} - H^{\bar{d}}] + \frac{3}{4}\, x^{-1} H^g \Big)$
$K^{*+}\Lambda$	$-\frac{1}{\sqrt{6}}\Big(2[2H^u - H^d - H^s] - [2H^{\bar{u}} - H^{\bar{d}} - H^{\bar{s}}] \Big)$
$K^{*+}\Sigma^0$	$-\frac{1}{\sqrt{2}}\Big(2[H^d - H^s] - [H^{\bar{d}} - H^{\bar{s}}] \Big)$
$K^{*0}\Sigma^+$	$[H^d - H^s] + [H^{\bar{d}} - H^{\bar{s}}]$
ϕp	$-\Big([H^s + H^{\bar{s}}] + \frac{3}{4}\, x^{-1} H^g \Big)$
$\pi^+ n$	$2[\tilde{H}^u - \tilde{H}^d] + [\tilde{H}^{\bar{u}} - \tilde{H}^{\bar{d}}]$
$\pi^0 p$	$\frac{1}{\sqrt{2}}\Big([2\tilde{H}^u + \tilde{H}^d] - [2\tilde{H}^{\bar{u}} + \tilde{H}^{\bar{d}}] \Big)$
$K^+\Lambda$	$-\frac{1}{\sqrt{6}}\Big(2[2\tilde{H}^u - \tilde{H}^d - \tilde{H}^s] + [2\tilde{H}^{\bar{u}} - \tilde{H}^{\bar{d}} - \tilde{H}^{\bar{s}}] \Big)$
$K^+\Sigma^0$	$-\frac{1}{\sqrt{2}}\Big(2[\tilde{H}^d - \tilde{H}^s] + [\tilde{H}^{\bar{d}} - \tilde{H}^{\bar{s}}] \Big)$
$K^0\Sigma^+$	$[\tilde{H}^d - \tilde{H}^s] - [\tilde{H}^{\bar{d}} - \tilde{H}^{\bar{s}}]$

full analogy. The integrals over meson distribution amplitudes in (8) can be expressed as

$$\int_0^1 dz\, \frac{1}{z(1-z)}\, \phi(z) = 6\Big[1 + \sum_{n=1}^{\infty} a_{2n}\Big], \qquad \int_0^1 dz\, \frac{2z-1}{z(1-z)}\, \phi(z) = 6 \sum_{n=1}^{\infty} a_{2n-1} \tag{10}$$

through their coefficients in the expansion

$$\phi(z) = 6z(1-z)\Big[1 + \sum_{n=1}^{\infty} a_n\, C_n^{3/2}(2z-1)\Big] \tag{11}$$

on Gegenbauer polynomials, where z is the light-cone momentum fraction carried by the quark in the meson. Note that odd Gegenbauer coefficients a_{2n-1} describe an asymmetry in the momentum distribution of the quark and antiquark in the meson. They can be nonzero for K and K^* due to flavor SU(3) breaking. In (8) to (11) we have not displayed the logarithmic dependence on the renormalization scale in α_s and on the factorization scale in the GPDs and the distribution amplitudes.

Using flavor SU(3) symmetry one can relate the transition GPDs from the proton to a hyperon to the distributions $H^q(x,\xi,t)$ for quark flavor q in the proton [4, 7]. This gives in particular $H_{p\to\Lambda} = -[2H^u - H^d - H^s]/\sqrt{6}$ and an analogous relation for $\tilde{H}_{p\to\Lambda}$. We use these relations throughout, except for $\tilde{E}$, where there are large effects of SU(3) breaking as we shall see below. Results analogous to (8) hold for all meson channels we consider, see e.g. [4, 6, 17], and we have collected the relevant combinations of GPDs in Table 1. There we have introduced $H^{\bar{q}}(x,\xi,t) = -H^q(-x,\xi,t)$

and $\tilde{H}^{\bar{q}}(x,\xi,t) = \tilde{H}^{q}(-x,\xi,t)$, so that for $x > 0$ we have simple forward limits

$$H^q(x,0,0) = q(x), \quad H^{\bar{q}}(x,0,0) = \bar{q}(x), \quad \tilde{H}^q(x,0,0) = \Delta q(x), \quad \tilde{H}^{\bar{q}}(x,0,0) = \Delta\bar{q}(x) \tag{12}$$

in terms of the unpolarized and polarized quark and antiquark densities in the proton. For gluons we have $H^g(x,0,0) = xg(x)$, which is the origin of the additional factors x^{-1} in the entries for ρ^0, ω, ϕ. In addition to the replacements in Table 1 one has of course to take the appropriate meson distribution amplitude and meson decay constants in (8). For the latter we will take $f_\pi = 131\,\text{MeV}$, $f_K = 160\,\text{MeV}$, and

$$f_\rho = 209\,\text{MeV}, \quad f_\omega = 187\,\text{MeV}, \quad f_\phi = 221\,\text{MeV}, \quad f_{K^*} = 218\,\text{MeV} \tag{13}$$

from [18].

For α_s in (8) we will take the one-loop running coupling at the scale Q^2, with three active quark flavors and $\Lambda_{\text{QCD}} = 200\,\text{MeV}$. This gives $\alpha_s = 0.34$ at $Q^2 = 2.5\,\text{GeV}^2$, where we will show most of our numerical results. We will not attempt more refined choices of renormalization scale, as were for instance explored in [19], since our principal use of the leading-order calculation will be to describe the *relative* size of cross sections for different exclusive channels.

3 Modeling the generalized parton distributions

For the calculation of exclusive cross sections we use simple models of GPDs. They have been developed in [20, 4] and been used in most phenomenological analyses so far. Our aim here is not to improve on these models, but instead to see by how much predictions can vary *within* the given framework. We take a factorizing t dependence for H and $\tilde{H}$,

$$\begin{aligned} H^q(x,\xi,t) &= H^q(x,\xi)\, F_1^p(t), & H^g(x,\xi,t) &= H^g(x,\xi)\, F_1^p(t), \\ \tilde{H}^q(x,\xi,t) &= \tilde{H}^q(x,\xi)\, G_A(t)/G_A(0), \end{aligned} \tag{14}$$

where $F_1^p(t)$ is the electromagnetic Dirac form factor of the proton and $G_A(t)$ the isovector axial form factor of the nucleon. A more refined version of the model would take different combinations of the proton and neutron form factors for H^u and H^d, but for the low values of t dominating integrated cross sections, $F_1^n(t)$ is much smaller than $F_1^p(t)$ and we simply neglect it. In this sense (14) is consistent with the sum rule for the first moment $\int dx\, H^q(x,\xi,t)$. The ansatz for $\tilde{H}^q$ is consistent with the sum rule for $\int dx\, \tilde{H}^q(x,\xi,t)$ to the extent that the (unknown) isoscalar axial form factor has the same t dependence as the isovector one. In our numerical evaluations we take the familiar parameterizations

$$F_1^p(t) = \frac{4m_p^2 - 2.8t}{4m_p^2 - t}\, \frac{1}{[1 - t/(0.71\,\text{GeV}^2)]^2}\,, \qquad \frac{G_A(t)}{G_A(0)} = \frac{1}{[1 - t/(1.05\,\text{GeV}^2)]^2}\,. \tag{15}$$

We note that for the gluon distribution H^g there is no reason a priori to take the electromagnetic form factor $F_1^p(t)$ in the ansatz (14). It turns out, however, that $F_1^p(t)$ is well approximated by a dipole form $F_1^p(t) = [1 - t/(0.98\,\text{GeV}^2)]^{-2}$ for t up to about $3\,\text{GeV}^2$ [21] and thus close to the two-gluon form factor advocated in [22].

It is rather certain that the ansatz (14) is too simple and can at best reflect the correct t dependence in a limited range of x and ξ [4, 21, 23]. For x and ξ in the valence region, say above 0.2, the decrease of GPDs with t is most likely less steep than the one of $F_1^p(t)$ and $G_A(t)$. Whereas there are phenomenological constraints of the t behavior of valence quark GPDs [21] and for gluons at small x

[22], the behavior for sea quarks is largely unknown, and sea quarks are important for the x_B region around 0.1 we will be mostly concerned with. Furthermore, the t dependence of meson production at moderate Q^2 is strongly affected by power corrections, as is for instance seen in the Q^2 dependence of the logarithmic slope $B = (\partial/\partial t) \log(d\sigma/dt)|_{t=0}$ for ρ^0 production at very high energies [24]. We note that our ansatz (14) gives a slope parameter $B \approx 4\,\mathrm{GeV}^2$, which may be quite realistic for x_B around 0.1. Furthermore, cross section ratios should be less affected by the insufficiency of our ansatz, since they are sensitive only to the relative t dependence of the contributions from different quark flavors and from gluons.

For the t independent functions in (14) we use the double distribution based ansatz of [20], whose ingredients are the usual parton densities at a given factorization scale μ and a so-called profile parameter b, where μ and b are to be regarded as free parameters of the model. Explicit expressions are given in App. A. We will not take into account the evolution of GPDs, which should not be too problematic since our numerical applications will stay within a rather narrow range of Q^2.

The modeling of the nucleon helicity-flip distributions E^q and E^g is still at an early stage of development, with the most advanced considerations focused on the valence quark domain [4, 21]. Fortunately, contributions from E enter the unpolarized meson production cross section (5) with prefactors that are quite small in the kinematics we are most interested in. Following the argumentation of [25] that E is not much larger than H for a given parton species, we hence neglect E altogether in our cross section estimates.

The distributions $\tilde{E}$ cannot be neglected since they receive contributions proportional to ξ^{-1} that compensate the kinematic prefactors in the cross section (6). We model them as

$$\begin{aligned}
\tilde{E}_{p\to n}(x,\xi,t) &= \frac{\theta(|x|\le\xi)}{2\xi}\,\phi_\pi\left(\frac{x+\xi}{2\xi}\right)\frac{2m_p f_\pi\, g_{\pi NN}}{m_\pi^2-t}\,\frac{\Lambda^2-m_\pi^2}{\Lambda^2-t}, \\
\tilde{E}_{p\to \Lambda}(x,\xi,t) &= \frac{\theta(|x|\le\xi)}{2\xi}\,\phi_K\left(\frac{x+\xi}{2\xi}\right)\frac{(m_p+m_\Lambda) f_K\, g_{KN\Lambda}}{m_K^2-t}\,\frac{\Lambda^2-m_K^2}{\Lambda^2-t},
\end{aligned} \tag{16}$$

where the distribution amplitudes ϕ are the same as those introduced above. For the coupling constants we take the value $g_{\pi NN} = 2m_p G_A(0)/f_\pi \approx 14.7$ from the Goldberger-Treiman relation and $g_{KN\Lambda} \approx -13.3$ from [26]. Continued to the points $t = m_\pi^2$ or $t = m_K^2$ in the unphysical region, the expressions (16) become the well-known results from pion or kaon exchange [26, 27, 28]. These can only be expected to be good approximations for t close to the squared meson masses, and for $-t$ of several $0.1\,\mathrm{GeV}^2$ are to be regarded as extrapolations. In (16) we have included form factors that cut off the $1/(m_M^2 - t)$ behavior of the pure pole terms when $-t$ becomes large. As default value for the cut-off mass we will take $\Lambda = 0.8\,\mathrm{GeV}$ [29] and study the sensitivity of results to the precise value of this parameter. We note that for $\Lambda = 0.6\,\mathrm{GeV}$ and $-t \le 1\,\mathrm{GeV}^2$ the above form of $\tilde{E}_{p\to n}$ differs by less than 15% from the corresponding term calculated in the chiral quark-soliton model as given in Eq. (4.39) of [28].

With this model for $\tilde{E}$ the longitudinal cross section for $\gamma^* p \to \pi^+ n$ takes the form

$$\begin{aligned}
\frac{d\sigma_L}{dt} &= \frac{\alpha_{em}}{Q^6}\frac{x_B^2}{1-x_B}\Bigg\{(1-\xi^2)|\tilde{\mathcal{H}}(\xi,t)|^2 - 2m_p\,\xi\,\mathrm{Re}\,\tilde{\mathcal{H}}(\xi,t)\; Q^2 F_\pi(Q^2)\,\frac{g_{\pi NN}}{m_\pi^2-t}\,\frac{\Lambda^2-m_\pi^2}{\Lambda^2-t} \\
&\qquad - \frac{t}{4}\left[Q^2 F_\pi(Q^2)\,\frac{g_{\pi NN}}{m_\pi^2-t}\,\frac{\Lambda^2-m_\pi^2}{\Lambda^2-t}\right]^2\Bigg\},
\end{aligned} \tag{17}$$

where

$$F_\pi(Q^2) = \frac{2\pi\alpha_s}{9}\frac{f_\pi^2}{Q^2}\left[\int_0^1 dz \frac{1}{z(1-z)}\,\phi_\pi(z)\right]^2 \tag{18}$$

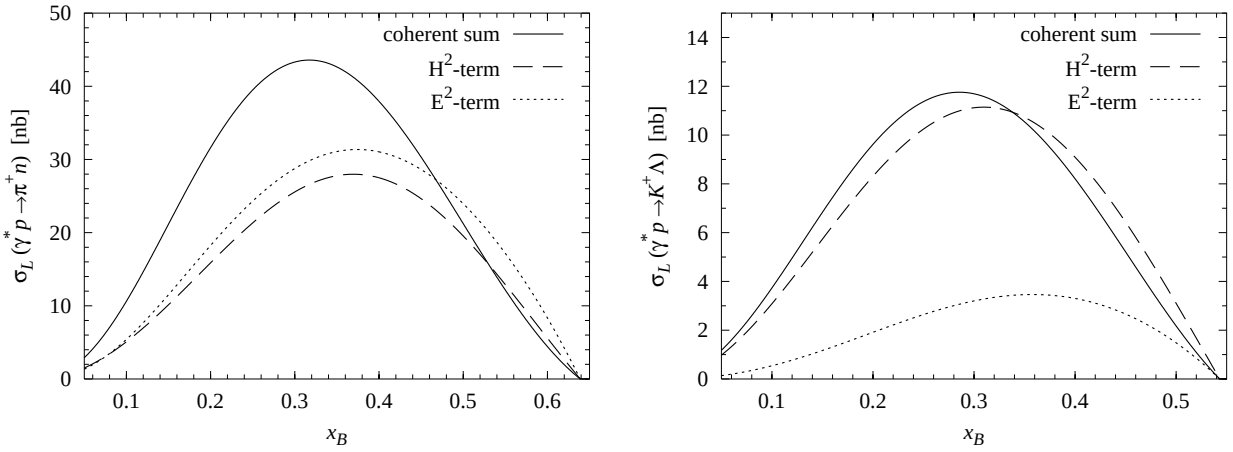

Figure 2: Leading-twist cross sections for $\gamma_L^* p \to \pi^+ n$ (left) and $\gamma_L^* p \to K^+ \Lambda$ (right) for $Q^2 = 2.5\,\mathrm{GeV}^2$. An upper cut on $-t$ of $1\,\mathrm{GeV}^2$ has been applied here and in all further plots of this paper. Shown are the individual contributions from $|\tilde{\mathcal{H}}|^2$ and $|\tilde{\mathcal{E}}|^2$, and their coherent sum according to (6).

is the electromagnetic pion form factor to leading order in α_s and $1/Q^2$. An similar expression involving $F_{K^+}(Q^2)$ is obtained for $\gamma^* p \to K^+ \Lambda$ according to (6) and (16). Note that the the $|\tilde{\mathcal{E}}|^2$ term in $d\sigma_L/dt$ has no x_B dependence other than from the explicit factor $x_B^2/(1-x_B)$. Within our model the $|\tilde{\mathcal{H}}|^2$ term reflects the behavior of the polarized parton distributions at momentum fractions of order ξ, and its contribution to $d\sigma_L/dt$ can very roughly be represented by $[\xi \Delta q(\xi)]^2$.

4 Exclusive pseudoscalar meson production

In this and the next section we present numerical results for cross sections of exclusive meson production. Our main focus is to compare the rates for different production channels and to investigate model uncertainties. Comparison with data in Sect. 6 will allow us to estimate the shortcomings of the leading approximation in $1/Q^2$ and in α_s, on which our calculations are based.

The factorization theorem for exclusive meson production requires t to be much smaller than Q^2. For definiteness we will give all meson cross sections in this paper integrated over $-t$ from its smallest kinematically allowed value $-t_0$ to an upper limit of $1\,\mathrm{GeV}^2$. In generalized Bjorken kinematics we have

$$-t_0 \approx \frac{2\xi^2(m_B^2 + m_p^2) + 2\xi(m_B^2 - m_p^2)}{1-\xi^2} \tag{19}$$

with ξ defined in (7). For low enough x_B most of the cross section should be accumulated in this t region, whereas for large x_B our cross sections decrease to the extent that $-t_0$ approaches $1\,\mathrm{GeV}^2$.

To begin with, let us investigate the relative importance of the contributions from $\tilde{\mathcal{H}}$ and $\tilde{\mathcal{E}}$ to π^+ and K^+ production with our model assumptions. As is seen in Fig. 2, exclusive π^+ production receives comparable contributions from both the $|\tilde{\mathcal{H}}|^2$ and the $|\tilde{\mathcal{E}}|^2$ term in (6), as well as from the interference term proportional to $\mathrm{Re}\,(\tilde{\mathcal{E}}^* \tilde{\mathcal{H}})$. Note that the relative weight of the contributions is different for $d\sigma_L/dt$, where it strongly depends on t given the characteristic t dependence of the pion pole term (16). In K^+ production the influence of $\tilde{\mathcal{E}}$ is less prominent, since the pole factor $(m_K^2 - t)^{-1}$ gives much less enhancement at small t than $(m_\pi^2 - t)^{-1}$.

To obtain the curves in Fig. 2 we have made a number of choices in the nonperturbative input to the cross section, which we now discuss in turn. In Fig. 3 we show how the cross section changes

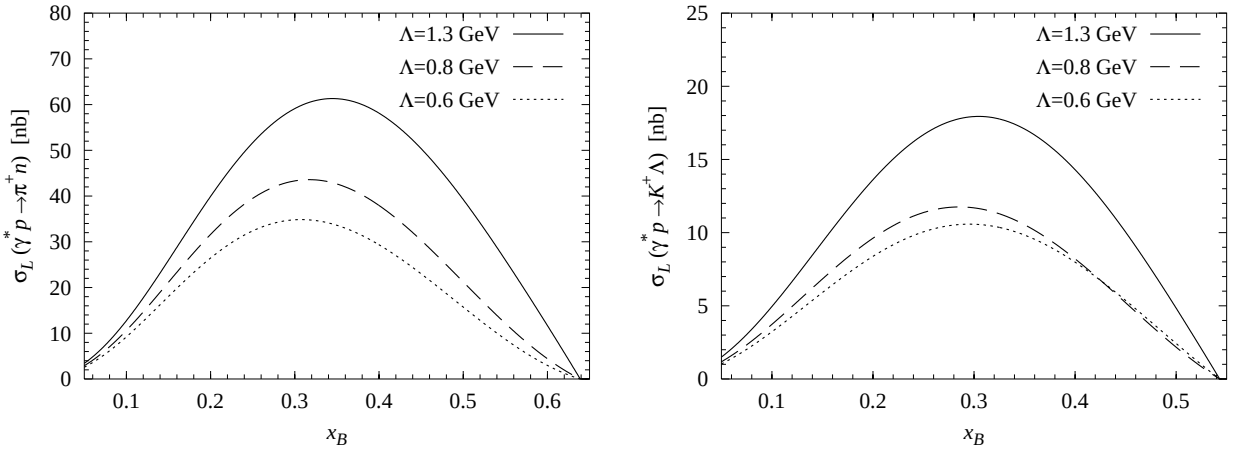

Figure 3: Leading-twist cross section for $\gamma_L^* p \to \pi^+ n$ (left) and $\gamma_L^* p \to K^+ \Lambda$ (right) at $Q^2 = 2.5\,\mathrm{GeV}^2$ obtained with different values of the parameter Λ in the form factor multiplying the pion or kaon pole contribution in (16).

when we vary the parameter Λ in our model for $\tilde{E}$, where $\Lambda = 1.3\,\mathrm{GeV}$ represents an upper limit of the values discussed in the phenomenological study [29], and $\Lambda = 0.6\,\mathrm{GeV}$ approximates the form factor dependence obtained for the pion pole contribution in [28], as discussed at the end of Sect. 2. Omitting the form factor altogether (tantamount to setting $\Lambda \to \infty$) the π^+ cross section would increase by more than a factor 1.4 and the K^+ cross section by more than a factor 1.7 compared with our default choice $\Lambda = 0.8\,\mathrm{GeV}$. Also, the cross sections would considerably increase when raising the upper cutoff in the $-t$ integration above $1\,\mathrm{GeV}^2$. In other words, the cross section would then receive substantial contributions from values of t far away from the region where the pion or kaon pole term can be regarded as a reasonable approximation of $\tilde{E}$.

For the pion distribution amplitude we have taken the asymptotic form $\phi_\pi(z) = 6z(1-z)$ under scale evolution, which is close to what can be extracted from data on the γ–π transition form factor, see e.g. [30, 31]. The study in [31] quotes limits on $a_2 + a_4$ at scale $\mu = 1\,\mathrm{GeV}$ of about ± 0.3 if all other Gegenbauer coefficients are set to zero. This corresponds to a change of the $\gamma^* p \to \pi^+ n$ cross section by a factor $(1 + a_2 + a_4)^2$ between 0.5 and 1.7. For the K^+ distribution amplitude we have taken the asymptotic form as well. Figure 4 shows how the K^+ cross section changes if instead one takes $a_1 = -0.05$ and $a_2 = 0.27$ at $\mu = 1\,\mathrm{GeV}$ from the QCD sum rule calculation [32]. This value of a_1 is compatible with the findings of [33].

For our model of $\tilde{H}$ we have taken a double distribution ansatz with a profile parameter $b = 1$ (see Sect. 2 and App. A). Taking $b = 2$ instead would decrease the K^+ cross section by a factor of approximately 0.6. The pion cross section changes less, because of the relative weight of $\tilde{\mathcal{H}}$ and $\tilde{\mathcal{E}}$. A more important source of uncertainty is however due to the polarized quark densities used as input to model $\tilde{H}$. As a default we have used the LO parameterization from [34] at a scale $\mu = 1\,\mathrm{GeV}$. Using instead the LO parameterization in scenario 1 of [35] at the same scale, the K^+ cross section changes as shown in Fig. 4. Note that any uncertainty on parton distributions is amplified in the meson production cross section, where GPDs appear squared.

Let us now comment on other pseudoscalar channels. The cross sections for $\gamma^* p \to K^+ \Sigma^0$ is about an order of magnitude smaller than the one for $\gamma^* p \to K^+ \Lambda$, as is seen in the numerical study of [26]. For the contribution from $\tilde{\mathcal{H}}$ this can be understood from the flavor structure in Table 1, where for a rough estimate one may concentrate on the dominant terms $\tilde{H}^u$ and $\tilde{H}^d$. For current parameterizations of polarized parton densities the combination $[2\tilde{H}^u - \tilde{H}^d]/\sqrt{3}$ for Λ production is

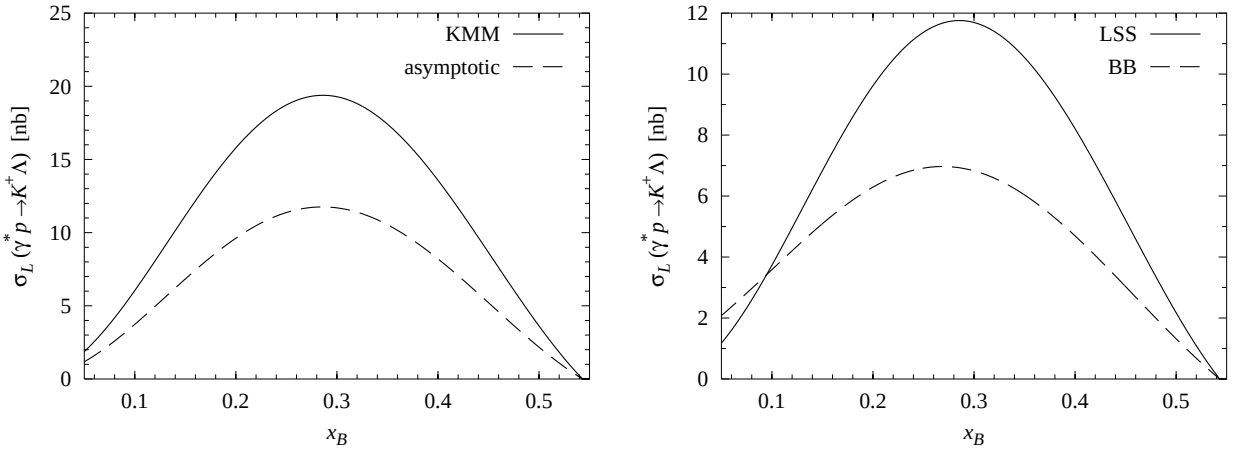

Figure 4: Left: Leading-twist cross section for $\gamma_L^* p \to K^+\Lambda$ at $Q^2 = 2.5\,\mathrm{GeV}^2$ calculated with the asymptotic kaon distribution amplitude and with the one from Khodjamirian, Mannel and Melcher (KMM) [32]. Right: The same cross section calculated with different parton distributions in the model for $\tilde{H}$. The distributions from Leader, Sidorov and Stamenov (LSS) [34] and from Blümlein and Böttcher (BB) [35] are taken at a scale $\mu = 1\,\mathrm{GeV}$.

clearly larger than $\tilde{H}^d$ in the analogous expression for the Σ^0 channel. Concerning the contribution from $\tilde{\mathcal{E}}$, the coupling $g_{KN\Sigma^0}$ is about three times smaller than $g_{KN\Lambda}$ appearing in (16), see [26]. Along the same lines one can see that the cross section for $\gamma^* p \to K^0\Sigma^+$ is of similar size as the one for $\gamma^* p \to K^+\Sigma^0$.

The channel $\gamma^* p \to \pi^0 p$ does not receive contributions from the pion pole term in (16) because of charge conjugation invariance, so that in our model it is entirely given by the contribution from $\tilde{\mathcal{H}}$. In Table 1 we see that the combination $2\tilde{H}^u + \tilde{H}^d$ for π^0 production is to be compared with $\sqrt{2}[\tilde{H}^u - \tilde{H}^d]$ for $\gamma^* p \to \pi^+ n$, which is of comparable size. One thus expects the π^0 cross section to be similar to the $|\tilde{\mathcal{H}}|^2$ part of the π^+ cross section.

The exclusive channels $\gamma^* p \to \eta p$ and $\gamma^* p \to \eta' p$ involve the combination $2\tilde{H}^u - \tilde{H}^d$ instead of $2\tilde{H}^u + \tilde{H}^d$ in the π^0 case, which is somewhat larger because the polarized distributions Δu and Δd have opposite sign. The strange quark contribution to these channels involves $\tilde{H}^s - \tilde{H}^{\bar{s}}$, which vanishes in our model with polarized parton distributions satisfying $\Delta s(x) = \Delta\bar{s}(x)$. A quantitative analysis requires the appropriate decay constants for the η and η', see for instance [36], but one can in general expect comparable cross sections for the π^0, η and η' channels.

5 Exclusive vector meson production

Within our model for the GPDs, the cross section for vector meson production is sensitive to unpolarized quark and gluon densities. To obtain an indication of uncertainties we have compared results with the LO distributions from CTEQ6 [37] and the LO distributions from MRST2001 [38]. For consistency we need LO rather than NLO parton densities, which unfortunately are not available in several of the most recent parton fits. We have checked that the NLO distributions from MRST2001 are in good agreement with those in the MRST2002 and MRST2004 analyses [39] for quark and antiquark densities down to about $x \sim 10^{-2}$ and for the gluon density down to about $x \sim 10^{-1}$. Comparing the LO distributions of CTEQ6 and MRST2001 at a scale $\mu^2 = 1.2\,\mathrm{GeV}^2$ (which is the lowest value accepted by the code for the MRST2001 parameterization) we find that the CTEQ6

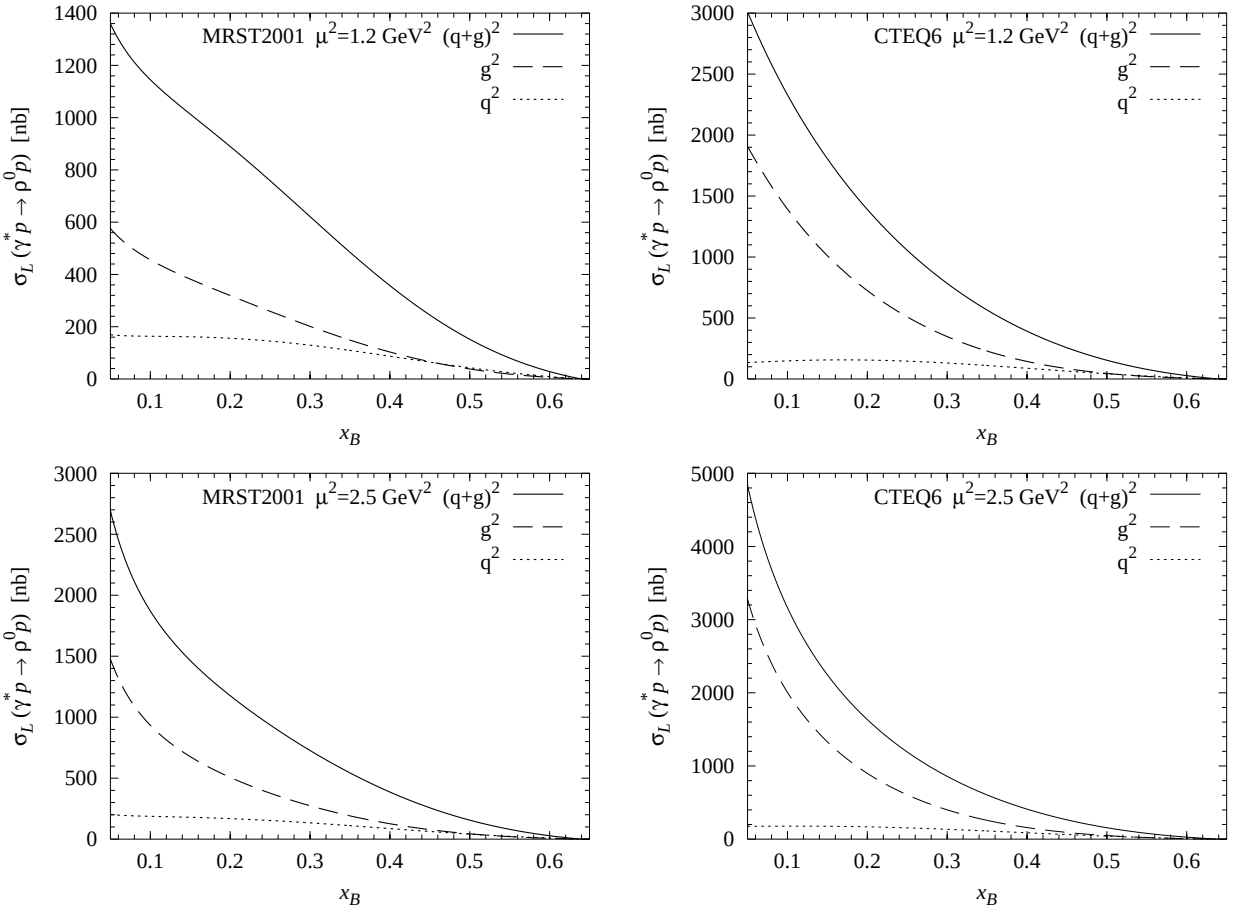

Figure 5: Leading-twist cross section for $\gamma_L^* p \to \rho^0 p$ at $Q^2 = 2.5\,\mathrm{GeV}^2$. Shown are the individual contributions from quark and gluon distributions and their coherent sum. The parton densities in the double distribution model are taken at scale $\mu^2 = 1.2\,\mathrm{GeV}^2$ for the upper and at $\mu^2 = 2.5\,\mathrm{GeV}^2$ for the lower plots.

gluon is larger for $x \lesssim 10^{-1}$ and smaller for $x \gtrsim 10^{-1}$. The u quark distribution is quite similar in the two sets for $x \gtrsim 10^{-2}$, whereas the s quark is significantly smaller for CTEQ6. The distributions for d, $\bar{u}$, $\bar{d}$ are quite similar for $x \gtrsim 10^{-1}$ and larger for CTEQ6 at smaller x. The LO parameterization of Alekhin [40] has significantly larger u and $\bar{u}$ distributions and a smaller gluon than the two other sets. At $\mu^2 = 1.2\,\mathrm{GeV}^2$ it has however almost no strange quarks in the proton, which we do not consider physically very plausible and which is in clear contrast with the results of CTEQ6, where a dedicated analysis of data constraining the strangeness distribution was performed. Since our study is crucially dependent on the flavor structure of parton distributions, we have therefore not used [40]. Comparing the different parton sets at the higher scale $\mu^2 = 2.5\,\mathrm{GeV}^2$ we find a very similar picture.

In the double distribution model of GPDs we take the profile parameter $b = 2$ for both quark and gluon distributions. For all mesons we take the asymptotic shape of the distribution amplitude, given that no direct experimental information is available for them. Theoretical estimates do not give stronger deviations from the asymptotic form than those we discussed for pseudoscalar mesons, see e.g. the compilation in [18]. In Fig. 5 we show the individual contributions from quark and gluon distributions to the ρ^0 cross section as well as their coherent sum. The clear difference between the CTEQ6 and MRST2001 result reflects the current uncertainty on the usual parton densities at low

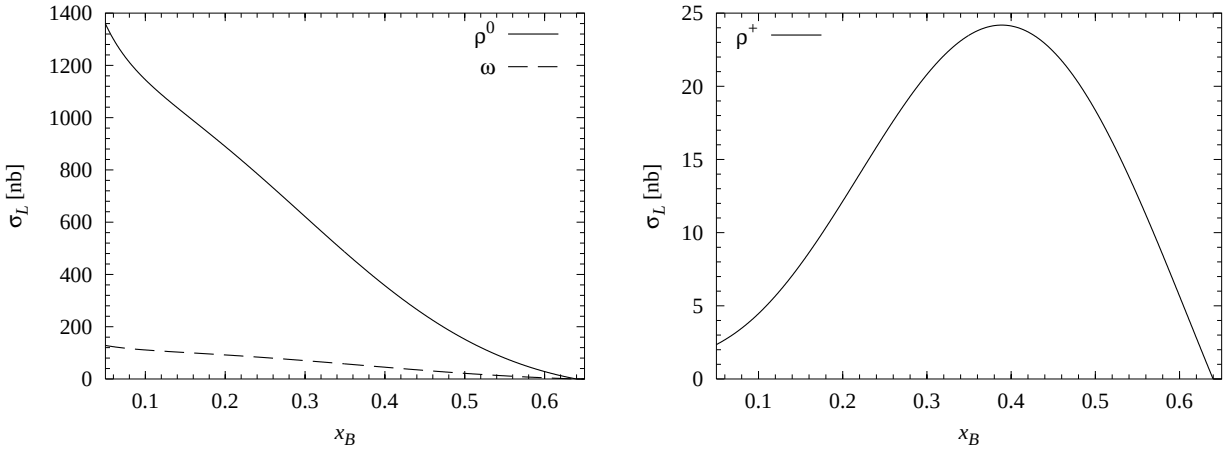

Figure 6: Leading-twist cross sections for $\gamma_L^* p \to \rho^0 p$ and $\gamma_L^* p \to \omega p$ (left) and for $\gamma_L^* p \to \rho^+ n$ (right) at $Q^2 = 2.5\,\mathrm{GeV}^2$, obtained with the MRST2001 parton densities taken at $\mu^2 = 1.2\,\mathrm{GeV}^2$.

scales in the relevant range of x. A striking feature is the clear dominance of the gluon distribution up to quite high values of x_B. Note that with our model of GPDs the convolutions $\mathcal{H}^q(\xi,t)$ and $\mathcal{H}^g(\xi,t)$ are sensitive to the forward parton distributions in a certain range of momentum fractions around ξ (see App. A). The strong dominance of gluon over quark distributions at small momentum fractions thus still shows its effect at x_B values above 10^{-1}. Note that we have taken the same t dependence for quark and gluon GPDs in our model (14), lacking phenomenological evidence to the contrary. Comparison of the t dependence e.g. for ρ^0 and ρ^+ production in equal kinematics could be of help here.

In our numerical calculations we have calculated the integrals (36) and (37) for the meson production amplitude with a lower cutoff at momentum fractions $x = 10^{-4}$. The cross section for $x_B = 0.05$ changes by less than 2% if we cut off at 10^{-5} or at 10^{-3}. It is diminished by about 10% with a cutoff at 0.005, which gives an indication of the relevance of momentum fractions which are an order of magnitude smaller than the x_B of the process in this model. Similar changes are observed for the individual quark and gluon distributions. We note that if we take a profile parameter $b = 1$ for quarks, the quark contribution to the cross section at $x_B = 0.05$ decreases by 10% when moving the cutoff on x from $x = 10^{-4}$ to $x = 10^{-3}$ and by 35% when moving it from $x = 10^{-4}$ to 0.005. Such a strong dependence on momentum fractions well below x_B seems difficult to understand in physical terms. We note that in the sea quark sector there are no strong theoretical arguments for taking $b = 1$, see Sect. 4.4 of [6].

In Fig. 5 we also observe a significant change of the gluon contribution to the cross section when changing the scale of the parton distributions in the double distribution ansatz (32). In contrast, the quark contribution changes by at most a factor of 1.3, reflecting the relatively weak scale evolution of quark and antiquark distributions compared with gluons in the relevant kinematic region. Changing the scale of the forward distributions in the double distribution model (32) gives a rough indication of how the actual GPDs evolve with μ^2 [20], so that the strong increase with μ^2 seen in Fig. 5 reflects a strong scale uncertainty of the leading-order approximation in α_s for channels involving gluon exchange. A full NLO analysis of meson production is possible using the results of [41] but beyond the scope of this work. We will use the smaller scale $\mu^2 = 1.2\,\mathrm{GeV}^2$ in our further studies, because the internal virtualities in the hard-scattering graphs of Fig. 1 are typically smaller than Q^2 (see also the study [46] of relevant scales in the small-x limit). Furthermore, the MRST2001 set gives a better description for the ratio of ϕ and ρ^0 production with our model (see below) and will hence

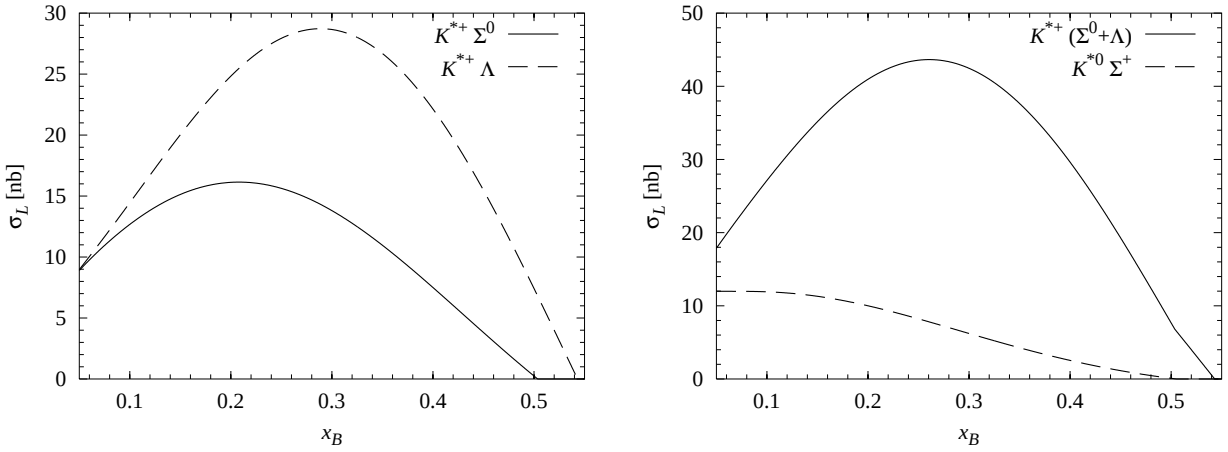

Figure 7: Leading-twist cross sections for $\gamma_L^* p \to K^{*+}\Lambda,\ K^{*+}\Sigma^0,\ K^{*0}\Sigma^+$ at $Q^2 = 2.5\,\mathrm{GeV}^2$, obtained with the MRST2001 parton densities taken at $\mu^2 = 1.2\,\mathrm{GeV}^2$.

be our default choice in the following.

In Fig. 6 we show the production cross sections for ρ^+, ρ^0 and ω. The x_B behavior of the ρ^+ cross section roughly follows the one of $\xi^2[u(\xi) - d(\xi) + \bar{u}(\xi) - \bar{d}(\xi)]^2$, which is a flavor nonsinglet combination and hence does not display the strong rise of sea quarks or gluons at small x. The clear suppression of ω production compared with the ρ^0 is a consequence of the relative factor in the gluon contribution (see Table 1) and at large x_B of the relative size of the flavor combination $2H^u - H^d$ compared with $2H^u + H^d$. We remark that the exclusive channel $\gamma^* p \to f_2\, p$ also contributes to semi-inclusive production of π^+, π^- and π^0. It involves the combination $2H^u + H^d - [2H^{\bar{u}} + H^{\bar{d}}]$, where sea quarks drop out, so that one may expect a cross section of similar size as for ρ^+ production. A numerical estimate would however require knowledge of quark and gluon distribution amplitudes of the f_2, see [42], and is beyond the scope of this work.

Figure 7 shows our results for K^{*+} and K^{*0} production. In contrast to K^+ production, the cross section for the Λ channel is not much larger than for the Σ^0 channel. Consulting Table 1 we see that this is because the contributions from u and d quarks partially cancel in $2H^u - H^d$ whereas they add in $2\tilde{H}^u - \tilde{H}^d$. We remark that the results for K^{*+} and K^{*0} production decrease by less than 25% when instead of MRST2001 we take the CTEQ6 parameterization. The uncertainty due to knowledge of the parton distributions is hence much less than for the gluon dominated channels.

Results for ϕ production are shown in Fig. 8. The dominance of the gluon over the strange quark contribution is clearly seen, although strange quarks are not entirely negligible with the MRST2001 parameterization.[1] Since gluons dominate for most x_B, we see the same trend concerning differences between the parameterizations and the choice of scale as for ρ^0 production. The ratio of σ_L for ϕ and ρ^0 production is shown in Fig. 9, where the dependence on μ^2 is seen to be much milder since it partially cancels in the ratio. The difference between CTEQ6 and MRST2001 is still significant and mainly due to the difference in the gluon distributions.

Preliminary data from HERMES [11, 13] give a ratio of about 0.08 for the cross sections of ϕ and ρ^0 production for $x_B = 0.09$ and $Q^2 = 2.46\,\mathrm{GeV}^2$ and for $x_B = 0.13$ and $Q^2 = 3.5\,\mathrm{GeV}^2$. These data contain a significant contribution from σ_T, and preliminary HERMES data [11, 12, 13] suggest that $R = \sigma_L/\sigma_T$ may be slightly smaller for ϕ than for ρ^0 production at the same Q^2. The ϕ to ρ^0 ratio for σ_L would then be somewhat larger than 0.08. In addition, one can expect that a narrower shape

[1] In the study [25] strange quarks were neglected based on inspection of the CTEQ6 parameterization.

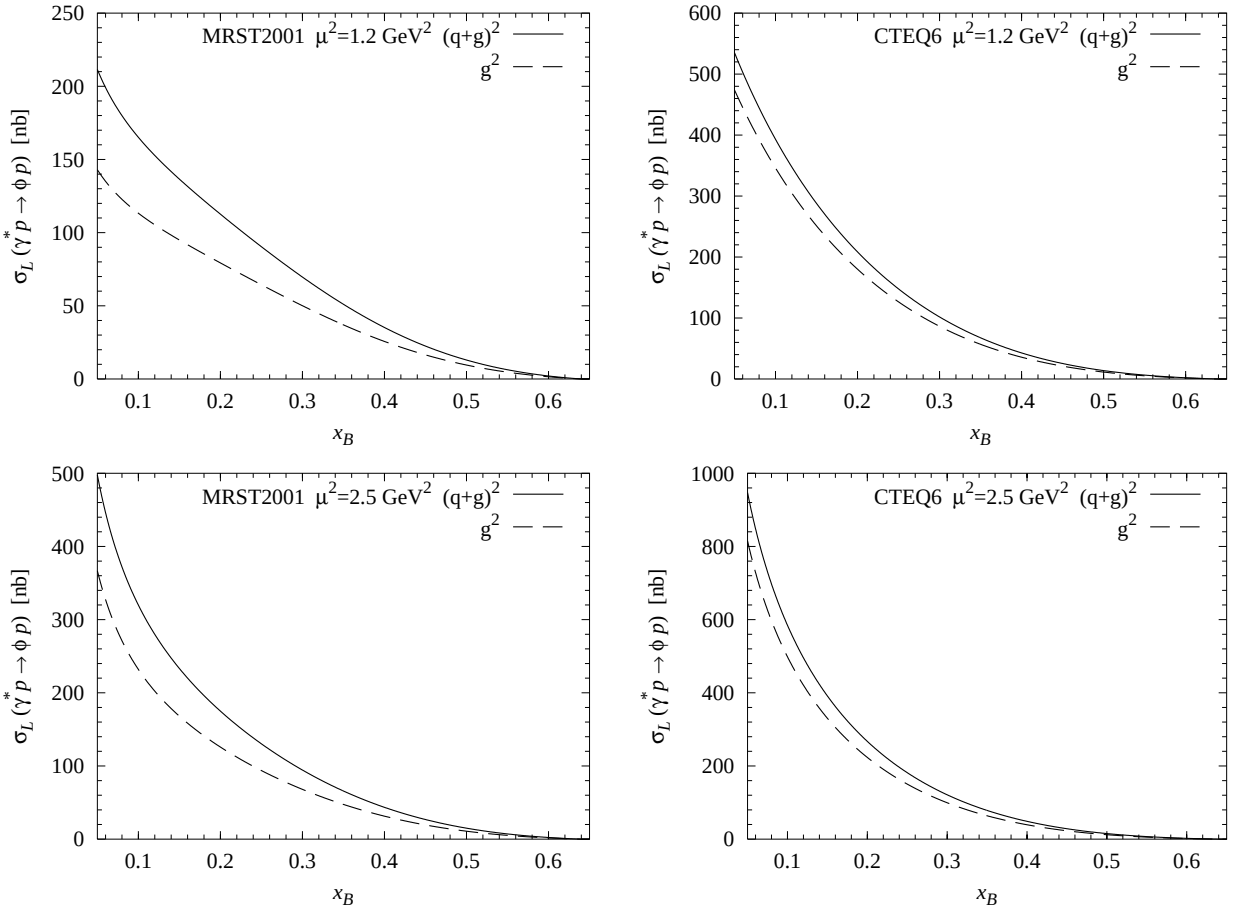

Figure 8: Leading-twist cross section for $\gamma_L^* p \to \phi p$ at $Q^2 = 2.5\,\mathrm{GeV}^2$. Shown are the individual contributions from gluons and the coherent sum of gluons and strange quarks. The upper plots are for parton densities taken at scale $\mu^2 = 1.2\,\mathrm{GeV}^2$ in the double distribution model, and the lower plots for parton densities taken at $\mu^2 = 2.5\,\mathrm{GeV}^2$.

of the distribution amplitude and power corrections due to the strange quark mass would decrease the estimates in Fig. 9 [25].

A complete representation of GPDs includes in addition to the double distribution the so-called D-term [43]. It vanishes in the forward limit $\xi = 0$ and does not affect the double distribution ansatz we are using. Its contribution to the GPDs can be expanded in Gegenbauer polynomials as

$$\begin{aligned} H_D^q(x,\xi,t) &= \theta(|x| \le \xi) \left(1 - \frac{x^2}{\xi^2}\right) \sum_{n=0}^{\infty} d_{2n+1}^q(t)\, C_{2n+1}^{3/2}\Big(\frac{x}{\xi}\Big), \\ H_D^g(x,\xi,t) &= \theta(|x| \le \xi)\, \frac{3\xi}{2} \left(1 - \frac{x^2}{\xi^2}\right)^2 \sum_{n=0}^{\infty} d_{2n+1}^g(t)\, C_{2n}^{5/3}\Big(\frac{x}{\xi}\Big) \end{aligned} \tag{20}$$

for $\xi > 0$. Such terms contribute to the real part of the convolution integrals needed in the meson production amplitudes as

$$I_D^q = \int_{-1}^{1} dx\, \frac{H_D^q(x,\xi,t)}{\xi - x - i\epsilon} = \int_{-1}^{1} dx\, \frac{H_D^{\bar q}(x,\xi,t)}{\xi - x - i\epsilon} = 2 \sum_{n=0}^{\infty} d_{2n+1}^q(t)\,,$$

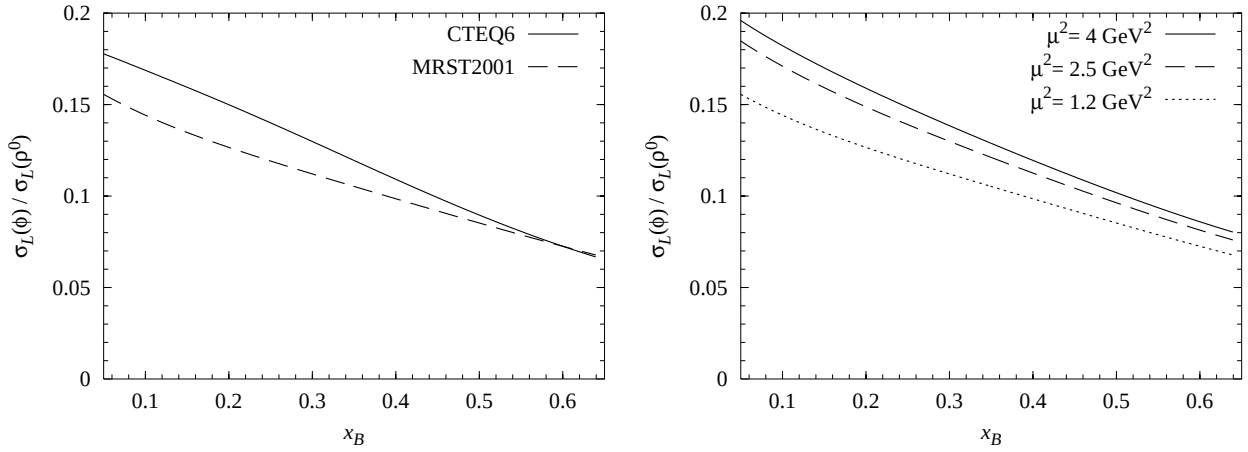

Figure 9: Ratio of leading-twist longitudinal cross sections for ϕ and ρ^0 production, obtained with different parton distributions taken at $\mu^2 = 1.2\,\mathrm{GeV}^2$ (left) and with the MRST2001 distribution taken at different μ^2 (right).

$$I_D^g \;=\; \int_{-1}^{1} dx\, \frac{H_D^g(x,\xi,t)}{x}\, \frac{1}{\xi - x - i\epsilon} \;=\; 2 \sum_{n=0}^{\infty} d_{2n+1}^g(t)\,. \tag{21}$$

These terms give a ξ independent contribution to $\mathcal{H}(\xi,t)$, in contrast to the contributions from the double distribution part, which very roughly follow the behavior of $\xi q(\xi)$, $\xi \bar{q}(\xi)$ or $\xi g(\xi)$ and hence grow as ξ becomes smaller. In [44] the first three coefficients in the quark D-term at $t = 0$ have been extracted from a calculation in the chiral quark-soliton model of the nucleon, giving $d_1^u(0) \approx -2.0$, $d_3^u(0) \approx -0.6$, $d_5^u(0) \approx -0.2$ and equal values for d quarks, referring to a scale μ of a few GeV [45]. The gluon D-term is parametrically subleading at the low scale intrinsic to the model, but evolution to μ of a few GeV can give values similar in size to those for quarks. The values $I_D^u = I_D^d = -5.6$ turn out to be similar in size and opposite in sign to the real parts of the corresponding integrals from the double distribution part in our model. The effect of such a D-term is however much weaker on the square $|\mathcal{H}|^2$ appearing the cross section, which is dominated by the imaginary parts of the integrals in a large region of x_B. Taking the above values for the quark D-term and $I_D^g = -11.2$ as an order-of-magnitude estimate, we find that the change of the various vector meson cross sections is at the 10% level for $x_B = 0.1$ and not more than a factor 1.5 in either direction for x_B below 0.3, where for definiteness we have taken the MRST2001 distributions at $\mu^2 = 1.2\,\mathrm{GeV}^2$.

6 Comparison with data and discussion of power corrections

Our calculation of meson production cross sections is based on the leading-twist approximation. It is known that corrections in $1/Q^2$ to leading-twist meson cross sections can be substantial for Q^2 of a few GeV^2. A systematic treatment of such power corrections remains an unsolved problem. There is however a number of approaches that allow one to model particular sources of power corrections, see e.g. [6] for a discussion and references. For vector meson production, a considerable suppression of the leading-twist result at moderate Q^2 is found when including in the hard-scattering kernel the transverse momentum of the quarks in the meson [46, 47, 48]. This means that the transverse resolution power of the virtual photon cannot be neglected compared with the transverse size of the meson. Similarly, the finite transverse momentum of the partons coming from the proton gives rise to power corrections, when it is included in the hard-scattering kernel. Estimating both effects in

Table 2: Experimental values $\sigma_L^{\rm exp}$ of the longitudinal cross section for the production of ρ^0 [10] and ϕ [11, 13, 49] from HERMES, and the ratio between our leading-twist results $\sigma_L^{\rm thy}$ (obtained with the MRST2001 distributions taken at $\mu^2 = 1.2\,{\rm GeV}^2$) and the data. The data for ϕ production is preliminary.

$\gamma^* p \to \rho^0 p$			
$Q^2[\,{\rm GeV}^2]$	x_B	$\sigma_L^{\rm exp}[\mu{\rm b}]$	$\sigma_L^{\rm thy}/\sigma_L^{\rm exp}$
2.3	0.1	0.21 ± 0.04	7.1
2.3	0.075	0.21 ± 0.04	7.6
4.0	0.16	0.09 ± 0.02	2.1
4.0	0.12	0.06 ± 0.01	3.5

$\gamma^* p \to \phi p$ (preliminary data)			
$Q^2[\,{\rm GeV}^2]$	x_B	$\sigma_L^{\rm exp}[{\rm nb}]$	$\sigma_L^{\rm thy}/\sigma_L^{\rm exp}$
2.3	0.087	15.6 ± 3.1	14.9
3.8	0.136	6.2 ± 1.24	5.5

a calculation considering only quark GPDs [47], a suppression of the leading-twist cross section for ρ^0 production by factors of 3.3, 4.9 and 9.2 was found at $Q^2 = 5\,{\rm GeV}^2$ for $x_B = 0.3$, 0.45 and 0.6, respectively. The recent study [48] for small x_B, where only gluon GPDs were retained and only the transverse quark momentum in the meson was taken into account, found corresponding suppression factors of 4.6 and 6.6 for respective values of $x_B = 2.95 \times 10^{-3}$ and 10^{-4} at $Q^2 = 4.8\,{\rm GeV}^2$. For $Q^2 = 10.9\,{\rm GeV}^2$ and $x_B = 4.3 \times 10^{-3}$ this factor decreases to 1.9. The discrepancy of the calculation including power suppression and experimental data is less than 35% in all three cases.[2]

In Table 2 we compare our leading-oder results for ρ^0 and ϕ production with data from HERMES [10, 11, 13, 49]. The discrepancy between our calculation and the ρ^0 data is well in the range of what can be explained by suppression from quark transverse momentum (considering in addition the uncertainties of our model for the GPDs). The stronger discrepancy with the ϕ data corresponds to our overestimating the ϕ to ρ^0 production ratio, discussed in the previous subsection.

The CLAS collaboration has published results for ρ^0 production at $x_B = 0.31$ and at $x_B = 0.38$, with Q^2 values between 1.5 and $2.3\,{\rm GeV}^2$ [14], and for ϕ production at $x_B = 0.29$ and $Q^2 = 1.7\,{\rm GeV}^2$ [50]. We consider that this kinematics, where the hadronic invariant mass W is below 2.3 GeV, is too close to threshold for comparison with a leading-twist calculation. A recent CLAS measurement [51] of ω production at higher energies, with Q^2 up to $5.1\,{\rm GeV}^2$ and W up to 2.8 GeV, found that helicity conservation between the γ^* and the ω is strongly violated, in contrast with the predicted behavior in the large-Q^2 limit. This prevented the extraction of σ_L and was ascribed to a strong contribution from π^0 exchange (which is absent in the ρ^0 and ϕ channels).

Let us now turn to π^+ production, where the situation is quite different. For the contribution from $\tilde{\mathcal{H}}$ one expects a similar suppression from quark transverse momentum as in the case of $\mathcal{H}$ in vector meson production, which was indeed found in the numerical study [47]. The pion exchange contribution from $\tilde{\mathcal{E}}$ is described in terms of the pion form factor according to (17), and this relation persists beyond the leading approximation in $1/Q^2$ to the extent that the pion emitted from the nucleon is not too far from off-shell. The power corrections for $\tilde{\mathcal{E}}$ are then the same as those for the pion form factor. The leading-twist expression (18) for $F_\pi(Q^2)$, with our choice of α_s specified after (13), undershoots the data of [52] by a factor 0.53 at $Q^2 = 1\,{\rm GeV}^2$ and a factor 0.41 at $Q^2 = 1.6\,{\rm GeV}^2$.

[2] The leading-order formula (90) in [48] with which we obtained the suppression factors just quoted contains in addition an approximation for small x_B, which should however not be the dominant effect comparing to the full calculation.

For $Q^2 = 3.3\,\mathrm{GeV}^2$ we find this factor to be between 0.34 and 0.77 within the large error bars in [53]. We will not attempt here to summarize the detailed theoretical and phenomenological work on the pion form factor, but remark that in addition to the leading-twist perturbative contribution there is a contribution from the Feynman mechanism, where the photon hits a quark carrying almost all of the pion momentum. This leads to a considerable enhancement over the leading-twist approximation. The calculations of $F_\pi(Q^2)$ in [54], which take this effect into account using different methods, give for instance results larger than our leading-twist value by factors between 2 and 4, even at $Q^2 = 10\,\mathrm{GeV}^2$. Note that these factors are to be squared in the contribution of $|\tilde{\mathcal{E}}|^2$ to the π^+ production cross section. For the production of the neutral pseudoscalars π^0, η, η', where there is no pion exchange contribution, one expects that power corrections will decrease the cross section, similarly to the case of vector meson production.

We have further compared our leading-twist calculation of $\epsilon\sigma_L$ for $\gamma^* p \to \pi^+ n$ with preliminary data on $\sigma_T + \epsilon\sigma_L$ from HERMES [55]. The HERMES data are presented for three different bins in x_B, with the average values of Q^2 and x_B for individual data points ranging from $1.5\,\mathrm{GeV}^2$ and 0.1 to $4.2\,\mathrm{GeV}^2$ and 0.17 in the first bin, from $2.5\,\mathrm{GeV}^2$ and 0.21 to $6.3\,\mathrm{GeV}^2$ and 0.25 in the second bin, and from $4.5\,\mathrm{GeV}^2$ and 0.34 to $10.5\,\mathrm{GeV}^2$ and 0.45 in the third bin [56]. Averaging the ratio between theoretical and experimental cross sections for the data points in each bin, we find ratios of 0.42, 0.19 and 0.12 in the first, second and third bin, respectively. The large discrepancy at large Q^2 and large x_B (which are strongly correlated in the data) is striking, but not too surprising given the size of corrections just estimated for the pion form factor. The much better agreement at smaller Q^2 and x_B might be accidental, given that we expect comparable contributions from $\tilde{\mathcal{H}}$ and $\tilde{\mathcal{E}}$, for with the power corrections go in different directions. Help in clarifying this issue could come from the spin asymmetry for transverse target polarization, which gives access to the relative size of $\tilde{\mathcal{H}}$ and $\tilde{\mathcal{E}}$ [4].

The case of π^+ production (and also the findings in the ω channel mentioned above) show that there are specific power corrections which will not cancel in cross section ratios for different processes. The situation is however better for channels that are sufficiently similar, as the example of ρ^0 and ϕ production shows. Corrections due to quark transverse momentum (as well as the overall normalization uncertainty from the scale of α_s in our leading-order calculation) will tend to cancel in that case. We hence expect that the overall pattern of differences between various meson cross sections we estimated at leading order will not be overturned in a more realistic treatment, given that these differences are largely controlled by the relevant combinations of quark and gluon distributions.

7 Exclusive channels in semi-inclusive pion and kaon production

In semi-inclusive hadron production one considers processes of the type

$$e(k) \;+\; p(p) \;\;\to\;\; e(k') \;+\; h(q_h) \;+\; X, \tag{22}$$

where h is a specified hadron and X an unspecified inclusive final state. A basic observable is the distribution of the produced hadron over the variable

$$z = \frac{q_h p}{q p}, \tag{23}$$

which measures the fraction of the virtual photon energy carried by the produced hadron in the target rest frame. In the Bjorken limit of large Q^2 at fixed x_B and fixed z, semi-inclusive hadron production can be treated within a QCD factorization approach. The differential cross section factorizes into the distribution of partons of type i in the target, the cross section for the virtual photon scattering off this parton, and the fragmentation function $D^{i\to h}(z)$ describing the fragmentation of the struck

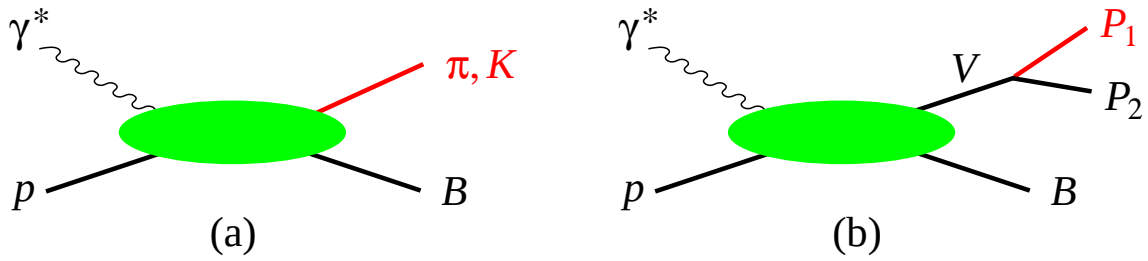

Figure 10: Contributions of exclusive channels to semi-inclusive pion and kaon production, calculated at leading order. (a) Direct exclusive production of pseudoscalar mesons. (b) Exclusive production of a vector meson with subsequent decay into pseudoscalars.

parton into the hadron h, which carries a fraction z of its longitudinal momentum. To leading order in α_s one has

$$\frac{d\sigma}{dQ^2\,dx_B\,dz} = 2\pi\alpha_{em}\,\frac{y^2}{1-\epsilon}\,\frac{1}{x_B Q^4}\,\sum_q e_q^2\left[q(x_B)D^{q\to h}(z) + \bar{q}(x_B)D^{\bar{q}\to h}(z)\right], \tag{24}$$

where the sum is over quark flavors. Note that (24) has the same Q^2-dependence as the inclusive DIS cross section in the Bjorken regime. The fragmentation functions are process-independent and describe not only semi-inclusive DIS but also e^+e^- annihilation into hadrons and the distribution of leading hadrons in high-p_T jets. Their scale evolution is governed by evolution equations analogous to the DGLAP equations for the parton distribution functions. Various parameterizations of the fragmentation functions have been presented in the literature, which fit e^+e^- annihilation and semi-inclusive DIS data at higher scales.

The derivation of semi-inclusive factorization relies on the fact that in the Bjorken limit the inclusive final state X has a large invariant mass

$$m_X^2 = Q^2\,\frac{1-z}{x_B} + m_p^2 - (q-q_h)^2, \tag{25}$$

and thus a large average multiplicity (note that the squared momentum transfer $(q-q_h)^2$ is always negative). The semi-inclusive cross section is thus obtained by summing over many individual channels. In practice m_X^2 is not very large for Q^2 values of a few GeV^2 typical of fixed-target experiments, for instance at Jefferson Lab or HERMES, especially at high z. At the same time, for moderate Q^2 the suppression of the cross sections for exclusive channels relative to the semi-inclusive cross section (see below) may not yet be effective. One thus can reach a situation in which the cross sections of individual exclusive channels becomes comparable to the semi-inclusive one. It is interesting to compare the semi-inclusive cross section (24) with the cross sections of exclusive channels contributing to semi-inclusive production. In the following we investigate the role of exclusive channels in semi-inclusive π and K production on a proton target. We study two types of exclusive channels (see Fig. 10) at a quantitative level:

i) direct exclusive production of pseudoscalar mesons, $\gamma^* p \to \pi^+ n$ and $\gamma^* p \to K^+\Lambda$,

ii) exclusive production of neutral or charged vector mesons ρ, ϕ, K^* with subsequent decay into pseudoscalars.

In the direct production of pseudoscalar mesons (Fig. 10a), the energy fraction z carried by the produced meson is related to the invariant momentum transfer to the nucleon t by

$$1 - z = x_B\,\frac{m_B^2 - m_p^2 - t}{Q^2} \tag{26}$$

according to (25). Exclusive production in the limit of large Q^2 at fixed x_B and fixed t thus corresponds to values of z very close to 1. For example, π^+ and K^+ production corresponds to $z > 0.94$ in typical HERMES kinematics of $x_B = 0.1$ and $Q^2 = 2.5\,\mathrm{GeV}^2$ with a maximum momentum transfer $|t| = 1\ \mathrm{GeV}^2$ (since the cross section drops rapidly with t, most events have z values yet closer to unity). Such exclusive contributions can usually be separated experimentally from the semi-inclusive events at smaller values of z.

The situation is different for the contribution to semi-inclusive production resulting from the decay of exclusively produced vector mesons (Fig. 10b). Since the decay products share the energy of the vector meson, such contributions result in an extended z distribution for the pion or kaon, even in the Bjorken limit. With the approximations described in Appendix B, the z spectrum of the pseudoscalar meson P_1 from the decay $V \to P_1 P_2$ can be written as

$$\frac{d\sigma(ep \to P_1 + P_2 B)}{dQ^2\, dx_B\, dz} = \frac{\alpha_{em}}{2\pi}\, \frac{y^2}{1-\epsilon}\, \frac{1-x_B}{x_B Q^2} \Big[\, \epsilon \sigma_L(\gamma^* p \to VB)\, D_L(z) + \sigma_T(\gamma^* p \to VB)\, D_T(z) \Big] \tag{27}$$

with

$$D_L(z) = \frac{3}{2\zeta^3}\,(z - z_0)^2, \qquad\qquad D_T(z) = \frac{3}{4\zeta^3}\,(z - z_1)(z_2 - z). \tag{28}$$

Here $z_1 \le z \le z_2$ with

$$z_0 = \frac{E_{P1}}{m_V}\,, \qquad\qquad z_1 = z_0 - \zeta\,, \qquad\qquad z_2 = z_0 + \zeta\,, \qquad\qquad \zeta = \frac{|\boldsymbol{q}_{P1}|}{m_V} \tag{29}$$

up to corrections of order $x_B\, m_p^2/Q^2$. For brevity we have not explicitly indicated the dependence of D_L and D_T on x_B and Q^2 due to these corrections. The energy and three-momentum of P_1 in the rest frame of the vector meson

$$\begin{aligned} E_{P1} &= \frac{m_V^2 + m_{P1}^2 - m_{P2}^2}{2m_V}, \\ |\boldsymbol{q}_{P1}| &= \frac{\sqrt{m_V^4 + m_{P1}^4 + m_{P2}^4 - 2\,(m_V^2 m_{P1}^2 + m_V^2 m_{P2}^2 + m_{P1}^2 m_{P2}^2)}}{2m_V} \end{aligned} \tag{30}$$

depend only on the meson masses, and so do z_0, z_1 and z_2 in the limit of large Q^2. In particular, the smallest and largest possible values of z for pions from the decay $\rho \to \pi\pi$ are $z_1 = 0.04$ and $z_2 = 0.96$ in that limit. The corresponding values for kaons from $\phi \to KK$ are $z_1 = 0.37$ and $z_2 = 0.63$. For the kaon from K^* decay one has $z_1 = 0.32$ and $z_2 = 0.96$, and for the pion from K^* decay one has $z_1 = 0.04$ and $z_2 = 0.68$.

According to (5), (6) and (27), the contribution of exclusive vector meson production to the cross section $d\sigma/(dQ^2\, dx_B\, dz)$ asymptotically scales as $1/Q^8$ at fixed x_B and z and is thus suppressed by $1/Q^4$ compared with the leading behavior (24) of the semi-inclusive cross section. Notice that (24) corresponds to transverse photon polarization, with contributions to the longitudinal cross arising at the level of α_s and of $1/Q^2$ corrections, just as in the familiar case of inclusive DIS. The situation is opposite for hard exclusive meson production, where σ_L dominates over σ_T in the large-Q^2 limit. Measurements show however that at Q^2 in the few GeV^2 region the ratio $R = \sigma_L/\sigma_T$ is still of order 1 in ρ^0 and ϕ production [11, 12, 13].

We first consider the semi-inclusive production of pions. Depending on the pion charge, exclusive channels contributing here are direct production $ep \to e\pi^+ n$ and the production and decay of ρ and $K^*(892)$. The ρ decays to almost 100% as $\rho^0 \to \pi^+\pi^-$ and $\rho^+ \to \pi^+\pi^0$, and the $K^*(892)$ decays to almost 100% into $K\pi$, with branching fractions

$$\begin{aligned} B(K^{*+} \to K^+\pi^0) &= \tfrac{1}{3}, \qquad & B(K^{*+} \to K^0\pi^+) &= \tfrac{2}{3}, \\ B(K^{*0} \to K^+\pi^-) &= \tfrac{2}{3}, \qquad & B(K^{*0} \to K^0\pi^0) &= \tfrac{1}{3} \end{aligned} \tag{31}$$

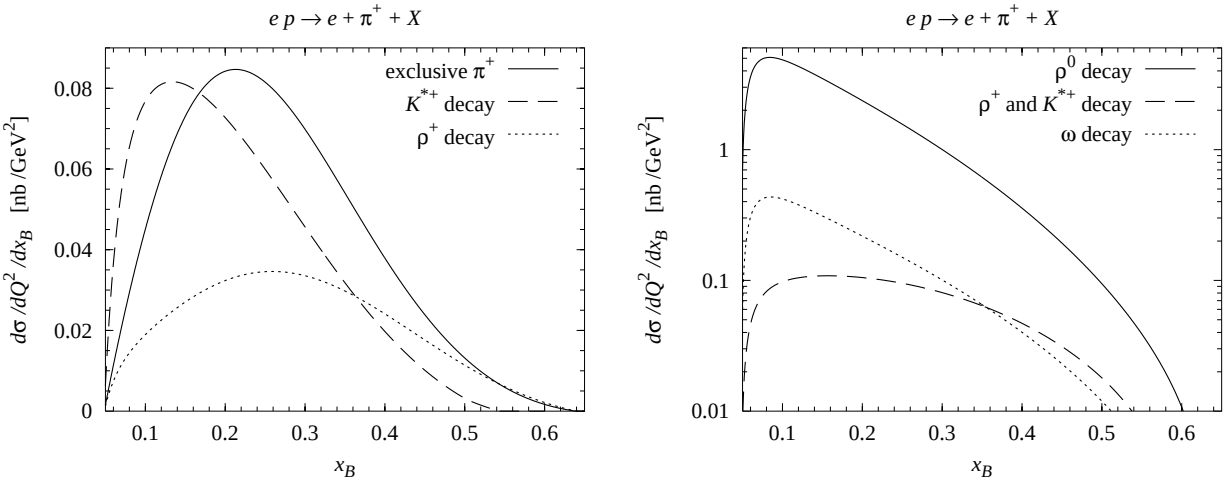

Figure 11: Exclusive contributions to the π^+ electroproduction cross section at $Q^2 = 2.5\,\mathrm{GeV}^2$, obtained from our leading-twist calculation of σ_L. This and the following plots are for a lepton beam energy of 27.5 GeV in the target rest frame. Left: direct exclusive production, and contributions from K^{*+} and ρ^+ decay. Right: sum of contributions from K^{*+} and ρ^+ decay compared with contributions from ω and ρ^0 decay.

following from isospin symmetry. Note that in quark fragmentation one has $\sigma(\pi^0) = \frac{1}{2}[\sigma(\pi^+)+\sigma(\pi^-)]$, which follows directly from the isospin relations between the pion fragmentation functions. This relation also holds for the contributions from K^* decay, but it is strongly violated for ρ decay. For the ρ^0 this effect was investigated in Ref. [8] in connection with the separation of $\bar{u}$ and $\bar{d}$ distributions in the proton using semi-inclusive DIS.

In Fig. 11 we show the result of our leading-twist calculation from Sects. 4 and 5 for the *ep* cross section of π^+ production. We give all *ep* cross section for a lepton beam energy of 27.5 GeV in the target rest frame, corresponding to the HERMES experiment, and recall that all our exclusive cross sections are calculated with an upper cutoff of $1\,\mathrm{GeV}^2$ on $|t|$. We see that the ρ^0 channel is clearly dominating. The ω, which decays to almost 100% into $\pi^+\pi^-\pi^0$, is much less prominent. According to our discussion in Sects. 4 and 6 one expects that the contribution from $ep \to e\pi^0 p$ to π^0 production is smaller than in the case of direct π^+ production. The same holds for the production and decay of η and η', which have several three-body decays contributing to all three pion channels. As we argued in Sect. 5 the production of $f_2(1270)$, which predominantly decays into $\pi^+\pi^-$ and $\pi^0\pi^0$, may contribute at a similar or lower level as ρ^+ decays. In Fig. 12 we show the z spectrum arising from different vector meson decays. Whereas ρ decays contribute in almost the entire z range, pions from K^* decays are limited to z values below 0.7. Note that due to charge conjugation invariance the z spectrum from ρ^0 decays is identical for the π^+ and π^-, and by isospin invariance the same holds for the π^+ and π^0 spectra from the decay of ρ^+. To illustrate the dependence of the z spectrum on the ratio R of longitudinal and transverse meson production cross sections we have taken values which correspond to the range measured in ρ^0 and ϕ production at $Q^2 = 2.5\,\mathrm{GeV}^2$ [11, 12, 13, 14].

We now compare the contribution from exclusive channels with the semi-inclusive cross section obtained from the leading-order expression (24) for quark fragmentation. We use the LO parton densities from MRST2001 and the LO fragmentation functions of Kretzer [58], both at a scale $Q^2 = 2.5\,\mathrm{GeV}^2$. Let us first take a look at the high-z tail of the spectrum, where direct exclusive production contributes. Integrating the semi-inclusive cross section for π^+ production for $z > 0.9$ at $Q^2 = 2.5\,\mathrm{GeV}^2$ and $x_B = 0.1$, we obtain $d\sigma/(dQ^2\,dx_B) = 0.19\,\mathrm{nb\,GeV}^{-2}$ from (24). This number should be

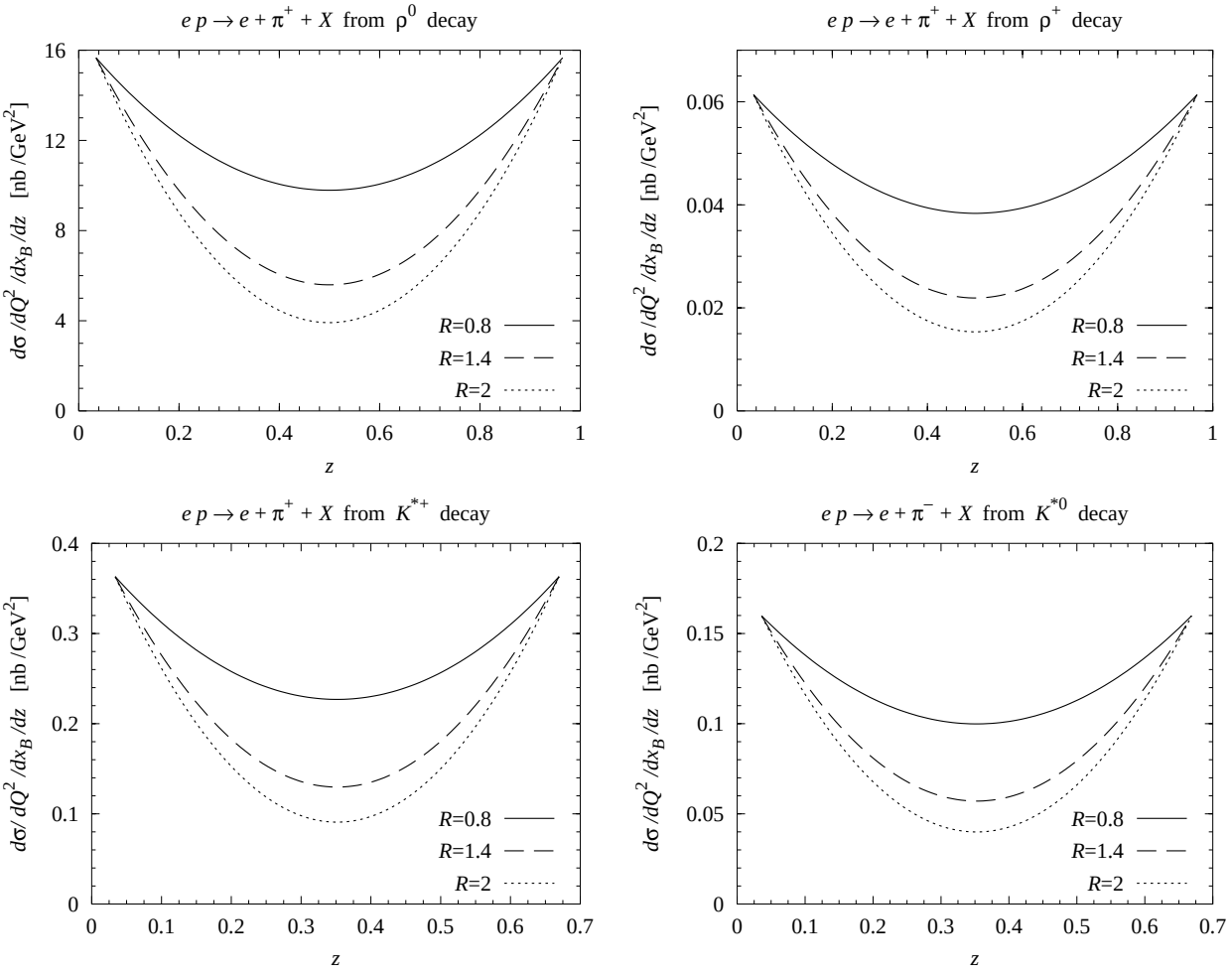

Figure 12: Contributions to the semi-inclusive pion electroproduction cross section from decays of exclusively produced vector mesons, for $Q^2 = 2.5\,\mathrm{GeV}^2$ and $x_B = 0.1$. Shown are the results corresponding to our leading-twist calculation of σ_L for vector meson production, and a value of $R = \sigma_L/\sigma_T$ chosen as indicated in the figure. Top left: π^+ from ρ^0 decay. Top right: π^+ from ρ^+ decay. Bottom left: π^+ from K^{*+} decay. Bottom right: π^- from K^{*0} decay. The contribution to π^0 production from K^{*+} and K^{*0} decays is given by the average of the corresponding curves in the two lower plots, according to (31).

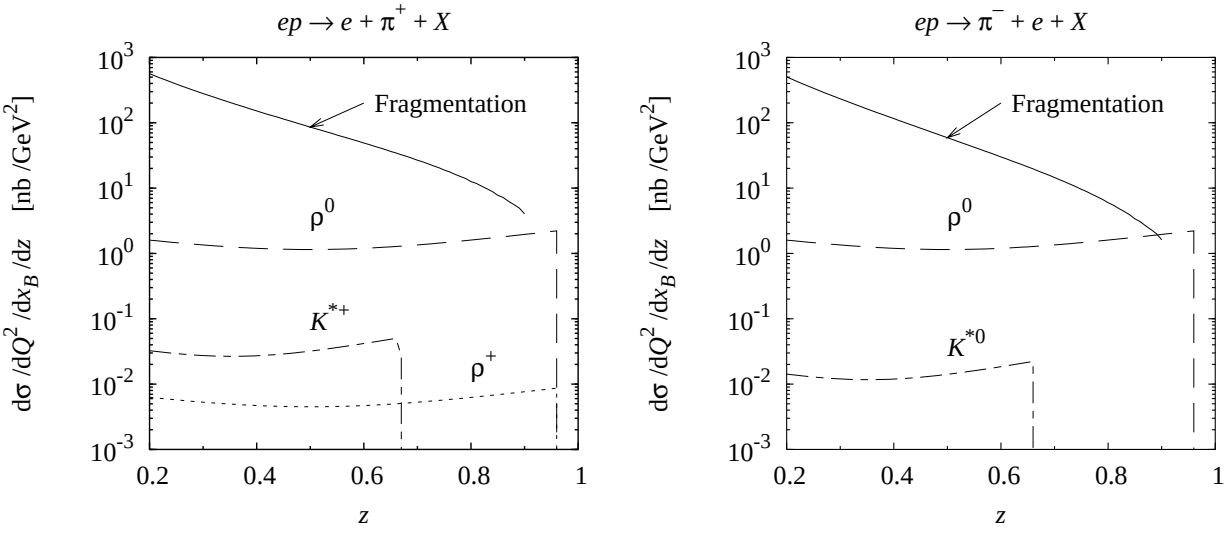

Figure 13: The cross section for semi-inclusive electroproduction of π^+ (left) and π^- (right), as a function of z, at $x_B = 0.1$ and $Q^2 = 2.5\,\mathrm{GeV}^2$. The cross sections from quark fragmentation were calculated using the LO fragmentation functions of Kretzer [58] and the MRST 2001 LO parton distributions. The contributions from vector meson decays were obtained by adjusting our leading–twist results for the vector meson production cross sections, as explained in the text. The value taken for the ρ^0 cross section matches the HERMES measurement [10].

understood as a naive extrapolation: the fragmentation functions are not well known for z close to 1, and in the above kinematics $z > 0.9$ corresponds to an invariant mass $m_X < 1.84\,\mathrm{GeV}$ according to (25), where leading-twist fragmentation can be just marginally valid. Our leading-twist result for $ep \to e\pi^+ n$ gives $d\sigma/(dQ^2\,dx_B) = 0.045\,\mathrm{nb\,GeV}^{-2}$, which according to our comparison with preliminary HERMES data (Sect. 6) undershoots the actual cross section by a factor of about 0.4. We thus find that for $z > 0.9$ direct exclusive pion production may be a substantial part of the semi-inclusive cross section, but cannot be more quantitative given the uncertainties just discussed.

For a realistic estimate of exclusive vector meson production we divide our leading-twist results for σ_L by a factor 7, except for ϕ production. According to Table 2 this brings us close to the HERMES measurement for ρ^0 production at $Q^2 = 2.3\,\mathrm{GeV}^2$ and $x_B = 0.1$, and according to our arguments in Sect. 6 it should give a reasonable estimate for the other channels. In other words, we assume that the ratio of vector meson channels is sufficiently well described by our leading-twist calculation. Only for ϕ production do we divide our leading-twist results by a different factor, namely by 15, following our comparison in Table 2 with preliminary HERMES data in this channel. One might argue that for the production of a K^*, which has one light and one strange quark, power corrections are between those for the ρ^0 and for the ϕ, but we refrain from such refinements here. Possible changes by a factor of 2 would in fact not change our conclusions regarding the role of K^* decays. For a prediction of σ_T we divide σ_L obtained as just described by the value $R = \sigma_L/\sigma_T = 1.2$ from preliminary HERMES data for ρ^0 production in the relevant kinematics [11, 12], except for the ϕ channel, where instead we take $R = 0.8$ from the parameterization of preliminary HERMES data in [11, 13]. Variation of R as shown in Fig. 12 would not affect the conclusions we shall draw.

Integrating the ρ^0 decay contribution to π^+ production for $z > 0.9$ at $Q^2 = 2.5\,\mathrm{GeV}^2$ and $x_B = 0.1$, we find $d\sigma/(dQ^2\,dx_B) = 0.13\,\mathrm{nb\,GeV}^{-2}$, which is surprisingly close to the extrapolation of the fragmentation result given above. The fragmentation formula for π^- production gives $d\sigma/(dQ^2\,dx_B) =$

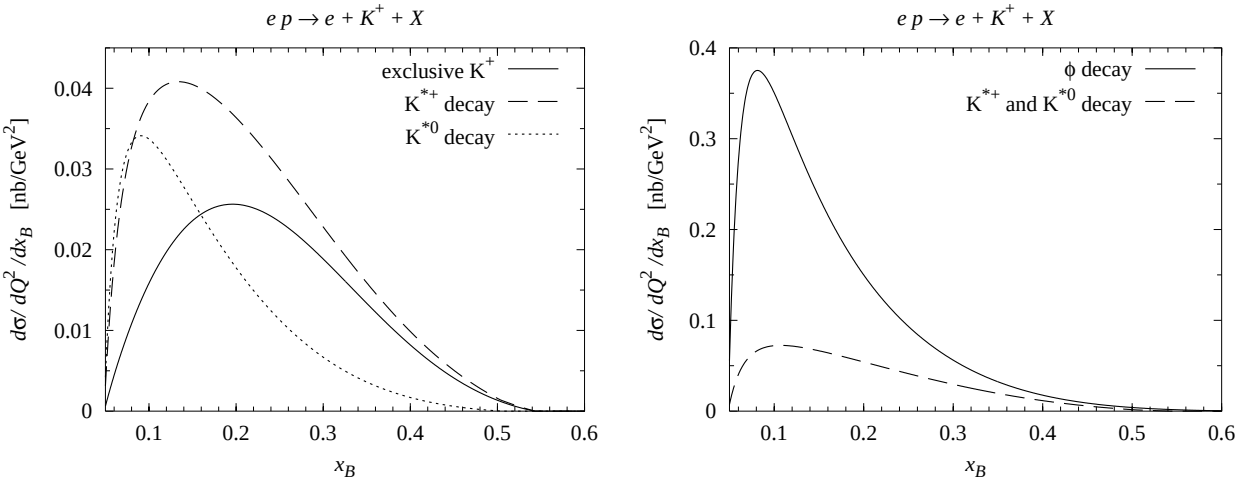

Figure 14: Same as Fig. 11, but for electroproduction of K^+.

$0.07\,\text{nb}\,\text{GeV}^{-2}$ when integrated over $z > 0.9$, so that in this case the ρ^0 contribution slightly overshoots the naive fragmentation result. In Fig. 13 we show the z spectrum of semi-inclusive π^+ and π^- production, comparing the fragmentation result with the contributions from vector meson decays. Following our above discussion we do not show the cross section from fragmentation for z above 0.9. We see that ρ^0 production gives a sizable contribution to semi-inclusive production for z greater than about 0.8. According to our estimate, ρ^+ production is suppressed relative to ρ^0 by two orders of magnitude and cannot compete with the cross section from quark fragmentation even at large z. The K^* decay contribution is somewhat larger in size but limited to z below 0.7. The fragmentation result for π^0 production is just the average of π^+ and π^- because of isospin invariance. With ρ^0 decay being absent and the contributions from other vector mesons being comparatively small, we find no exclusive channel that is prominent in semi-inclusive π^0 production for the kinematics discussed here. We expect direct exclusive production $ep \to e\pi^0 p$ to be much less important at high z than in the case of π^+ production, to the extent that power corrections enhance the π^+ but suppress the π^0 compared with the leading approximation in $1/Q^2$. Given the relative size of cross sections in Fig. 11 it is clear that pions from ω production are significantly smaller than the fragmentation result for all z, and we shall not analyze the kinematics of the corresponding three-body decay here.

Turning to semi-inclusive K^+ and K^- production, we show in Fig. 14 the contributions of the relevant exclusive channels to the ep cross section, obtained from our leading-twist calculation in Sect. 5. The production of ϕ, which decays to approximately 50% into K^+K^-, is clearly dominant for K^+ production, and it is the only channel contributing to K^- production. As is seen in the z-spectra of Fig. 15, it is however only the K^+ from K^* decays that extends to z values above 0.65.

Integrating the leading-order fragmentation formula (24) for K^+ production for $z > 0.9$ at $Q^2 = 2.5\,\text{GeV}^2$ and $x_B = 0.1$, we obtain $d\sigma/(dQ^2\,dx_B) = 0.048\,\text{nb}\,\text{GeV}^{-2}$, which is to be understood as an extrapolation as in the pion case discussed above. Our leading-twist estimate for direct exclusive K^+ production in Sect. 4 gives $d\sigma/(dQ^2\,dx_B) = 0.016\,\text{nb}/\,\text{GeV}^2$. Following our discussion in Sect. 6 one expects that power corrections will lead to weaker enhancement than in the case of $ep \to e\pi^+ n$ (or possibly even to a suppression), because $\tilde{\mathcal{H}}$ is more important in the leading-twist cross section for K^+ production than $\tilde{\mathcal{E}}$. Nevertheless, the above numbers suggest that direct exclusive K^+ production may be of some significance at the high-z end of the spectrum.

If we integrate the K^+ spectrum from K^{*+} and K^{*0} decays for $z > 0.9$, dividing our leading-twist result by 7 and accounting for the transverse cross section as described above, we obtain

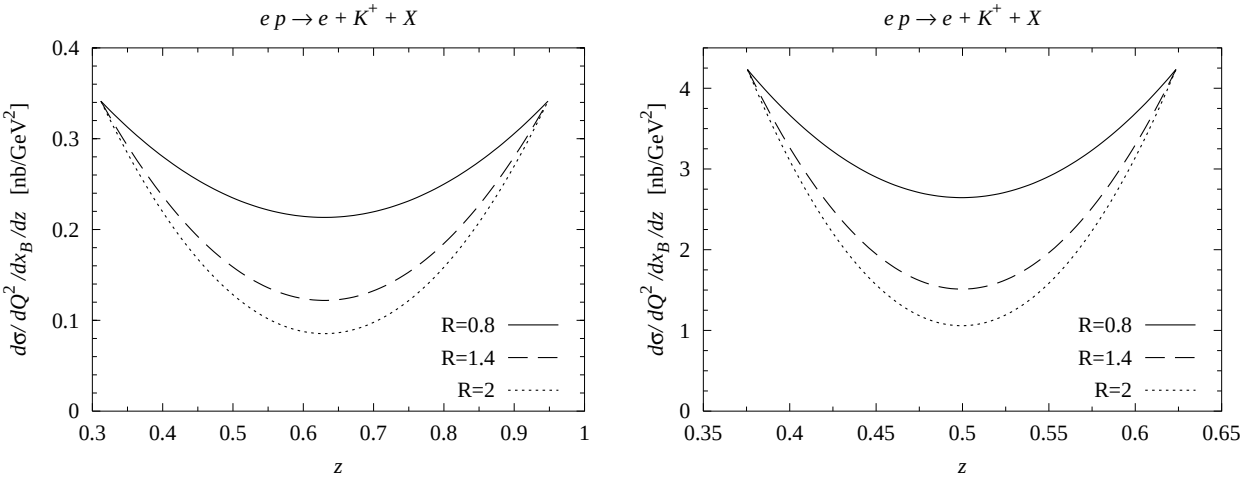

Figure 15: Same as Fig. 12, but for the contribution from K^{*+} and K^{*0} decays to K^+ production (left) and for the contribution of ϕ decay to K^+ or K^- production (right).

$d\sigma/(dQ^2\,dx_B) = 0.0021\,\text{nb}\,\text{GeV}^{-2}$, which is well below our extrapolation from leading-twist fragmentation. In Fig. 16 we compare the fragmentation result for semi-inclusive K^+ and K^- production with the individual contributions from K^* and ϕ decays. We conclude that, even within the uncertainties of our estimates, contributions from K^* production are only a fraction of the fragmentation result at any z, and that ϕ production, despite its larger cross section, is always well below the semi-inclusive cross section. Our finding concerning the ϕ contribution agrees with a recent study of measured kaon multiplicities in [9]. On one hand, kaon production by quark fragmentation is less suppressed compared with pion production than is exclusive ϕ production compared with production of ρ^0, and on the other hand ϕ decays only contribute in a z-range where the fragmentation functions are still large. Apart possibly from direct K^+ production at z close to 1, we thus find no exclusive channel dominating K^+ or K^- production in typical HERMES kinematics.

So far we have compared exclusive channels with quark fragmentation at $x_B = 0.1$ and $Q^2 = 2.5\,\text{GeV}^2$. We have also performed the comparison of Figs. 13 and 16 for $x_B = 0.3$ at the same Q^2. For the vector meson cross sections we used the same values of R and the same correction factors as for $x_B = 0.1$, dividing our leading-twist cross sections by 7 for all vector mesons except the ϕ, where we divide by 15. In doing this, we assume that the leading-twist approximation gives a realistic description of the x_B dependence in this region. We find that our qualitative conclusions do not change when going to the larger value of x_B.

A comment is in order concerning the treatment of exclusive channels in the analysis of semi-inclusive DIS data when extracting quark fragmentation or distribution functions. It is by no means clear that by subtracting contributions of individual exclusive channels from the total yield one obtains an observable more suitable for comparison with the quark fragmentation formulae. In fact, the derivation of factorization theorems relies on the sum over all channels X in (22) to be complete. At sufficiently large Q^2, each individual exclusive channel by itself is a power correction which may or may not be included in the leading-twist analysis. This situation is similar to the one with the contribution from individual nucleon resonances to the cross section of inclusive DIS. A way to think about the relation of exclusive channels to the leading-twist cross section is quark-hadron duality. It remains a challenge to formulate the problem of quark-hadron duality for semi-inclusive DIS in a quantitative fashion.

Symmetry properties like $\sigma(\pi^0) = \frac{1}{2}[\sigma(\pi^+)+\sigma(\pi^-)]$ can emerge from summing over many channels

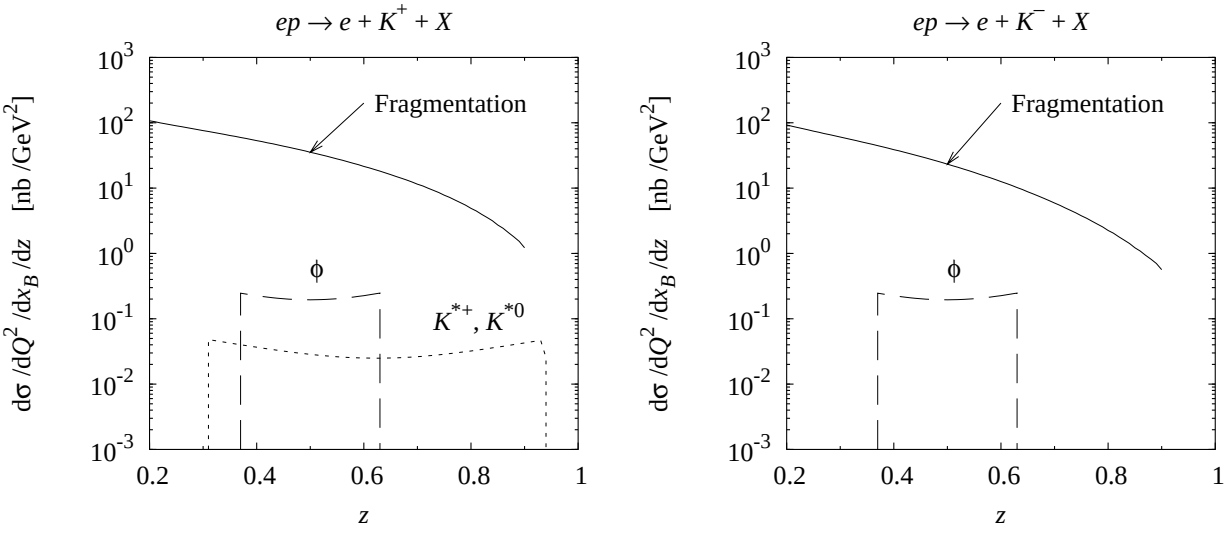

Figure 16: Same as Fig. 13, but for semi-inclusive production of K^+ (left) and K^- (right). As discussed in the text, the ϕ production cross section used in this plot matches the preliminary results of a HERMES measurement [11, 13].

which do not fulfill this relation individually. If however a single channel like ρ^0 production dominates the semi-inclusive cross section, it clearly becomes more and more difficult for the remaining channels to compensate the missing symmetry between charged and neutral pion production. In such a situation, parton-hadron duality must cease to work. The outcome of our study is that indeed the only channel whose contribution can become dangerously large in HERMES kinematics, is the ρ^0 contribution to π^+ and π^- production.

8 Summary

We have evaluated the cross section for a variety of exclusive meson production channels for moderate to large x_B at leading order in $1/Q^2$ and in α_s. Cross sections change significantly when varying the nonperturbative input, generalized parton distributions and meson distribution amplitudes, within plausible limits of current model building. On one hand this implies an uncertainty in predicting these cross sections, but on the other hand it implies that their measurement can ultimately help to constrain the nonperturbative functions, provided theoretical control over corrections to the leading-order formulae. We find the largest cross section uncertainties for ρ^0, ω and ϕ production, which is sensitive to the generalized gluon distribution over a large range of x_B, reflecting the current uncertainty of the unpolarized gluon density at low scales. A strong dependence on the factorization scale in these channels underlines the need for analysis at next-to-leading order in α_s. Comparing our leading-twist cross section with experimental data, we confirm that for Q^2 of a few GeV^2 power corrections are substantial. In particular, the suppression of vector meson cross sections we find is consistent with what has been estimated in the literature from the effects of parton transverse momentum in the hard-scattering subprocess. A consistent description of such effects together with next-to-leading order corrections in α_s remains a challenge for theory. As is seen for the ratio of ϕ and ρ^0 production, the most serious theoretical uncertainties cancel however in cross section ratios for sufficiently similar channels (the main distinction being between channels with and without t-channel pion exchange).

Rescaling our leading-twist cross sections such as to be consistent with experimental data for ρ^0 and ϕ production, we have compared their contribution to semi-inclusive pion or kaon production with the result of leading-twist quark fragmentation, focusing on the typical kinematics of HERMES measurements, where $Q^2 \sim 2.5\,\mathrm{GeV}^2$ and $x_B \sim 0.1$. Within large uncertainties, direct exclusive production of π^+ and possibly K^+ appears to be comparable with the fragmentation result extrapolated to the bin $0.9 < z < 1$. Through their decays, exclusively produced ρ, ϕ and K^* contribute in a wide range of z. Pions from K^* decay and kaons from ϕ decay are however limited to z below 0.7. With this and the relative size of cross sections, our estimates indicate that in typical HERMES kinematics the only exclusive channel whose cross section can compete with quark fragmentation is the ρ^0. The ρ^0 saturates the quark fragmentation result for semi-inclusive π^+ and π^- production at large z. Since the ρ^0 does not contribute to π^0 and to kaon production, there is no corresponding "dangerous" vector channel in these cases.

Acknowledgments

We are indebted to E.-C. Aschenauer, H. Avakian, A. Borissov, C. Hadjidakis, D. Hasch, A. Hillenbrand, M. Strikman, M. Vanderhaeghen and A. Vinnikov for valuable discussions and information. This work is supported by the Helmholtz Association, contract number VH-NG-004. This work is supported by U.S. Department of Energy Contract DE-AC05-84ER40150, under which the Southeastern Universities Research Association (SURA) operates the Thomas Jefferson National Accelerator Facility.

A Integrals over GPDs within the double distribution model

The t independent functions in the ansatz (14) for quark and gluon GPDs are modeled as

$$\begin{aligned}
H^q(x,\xi) &= \int_{-1}^{1} d\beta \int_{-1+|\beta|}^{1-|\beta|} d\alpha\; \delta(x-\beta-\xi\alpha)\, h(\beta,\alpha) \Big[\theta(\beta)\, q(\beta) \;-\theta(-\beta)\, \bar q(-\beta)\Big], \\
H^g(x,\xi) &= \int_{-1}^{1} d\beta \int_{-1+|\beta|}^{1-|\beta|} d\alpha\; \delta(x-\beta-\xi\alpha)\, h(\beta,\alpha)\, \beta \Big[\theta(\beta)\, g(\beta) \;-\theta(-\beta)\, g(-\beta)\Big], \\
\tilde H^q(x,\xi) &= \int_{-1}^{1} d\beta \int_{-1+|\beta|}^{1-|\beta|} d\alpha\; \delta(x-\beta-\xi\alpha)\, h(\beta,\alpha) \Big[\theta(\beta)\, \Delta q(\beta) + \theta(-\beta)\, \Delta \bar q(-\beta)\Big],
\end{aligned} \tag{32}$$

where θ denotes the usual step function, q, $\bar q$, Δq, $\Delta \bar q$ the unpolarized and polarized quark and antiquark distributions, and g the unpolarized gluon distribution. The profile function

$$h(\beta,\alpha) = \frac{\Gamma(2b+2)}{2^{2b+1}\Gamma^2(b+1)}\, \frac{[(1-|\beta|)^2-\alpha^2]^b}{(1-|\beta|)^{2b+1}} \tag{33}$$

depends on a parameter b, which we chose to be either $b = 1$ or $b = 2$ in this work.

For meson production amplitudes we need the integrals

$$\begin{aligned}
I^q(\xi) &= \int_{-1}^{1} dx\, \frac{H^q(x,\xi)}{\xi - x - i\epsilon}, & I^{\bar q}(\xi) &= \int_{-1}^{1} dx\, \frac{H^{\bar q}(x,\xi)}{\xi - x - i\epsilon} \;=\; [I^q(-\xi)]^*, \\
\tilde I^q(\xi) &= \int_{-1}^{1} dx\, \frac{\tilde H^q(x,\xi)}{\xi - x - i\epsilon}, & \tilde I^{\bar q}(\xi) &= \int_{-1}^{1} dx\, \frac{\tilde H^{\bar q}(x,\xi)}{\xi - x - i\epsilon} \;=\; -[\tilde I^q(-\xi)]^*,
\end{aligned} \tag{34}$$

where we used the definitions $H^{\bar q}(x,\xi) = -H^q(-x,\xi)$ and $\tilde H^{\bar q}(x,\xi) = \tilde H^q(-x,\xi)$ together with the fact that these functions are even in ξ. The required integral for gluons can be brought into the same

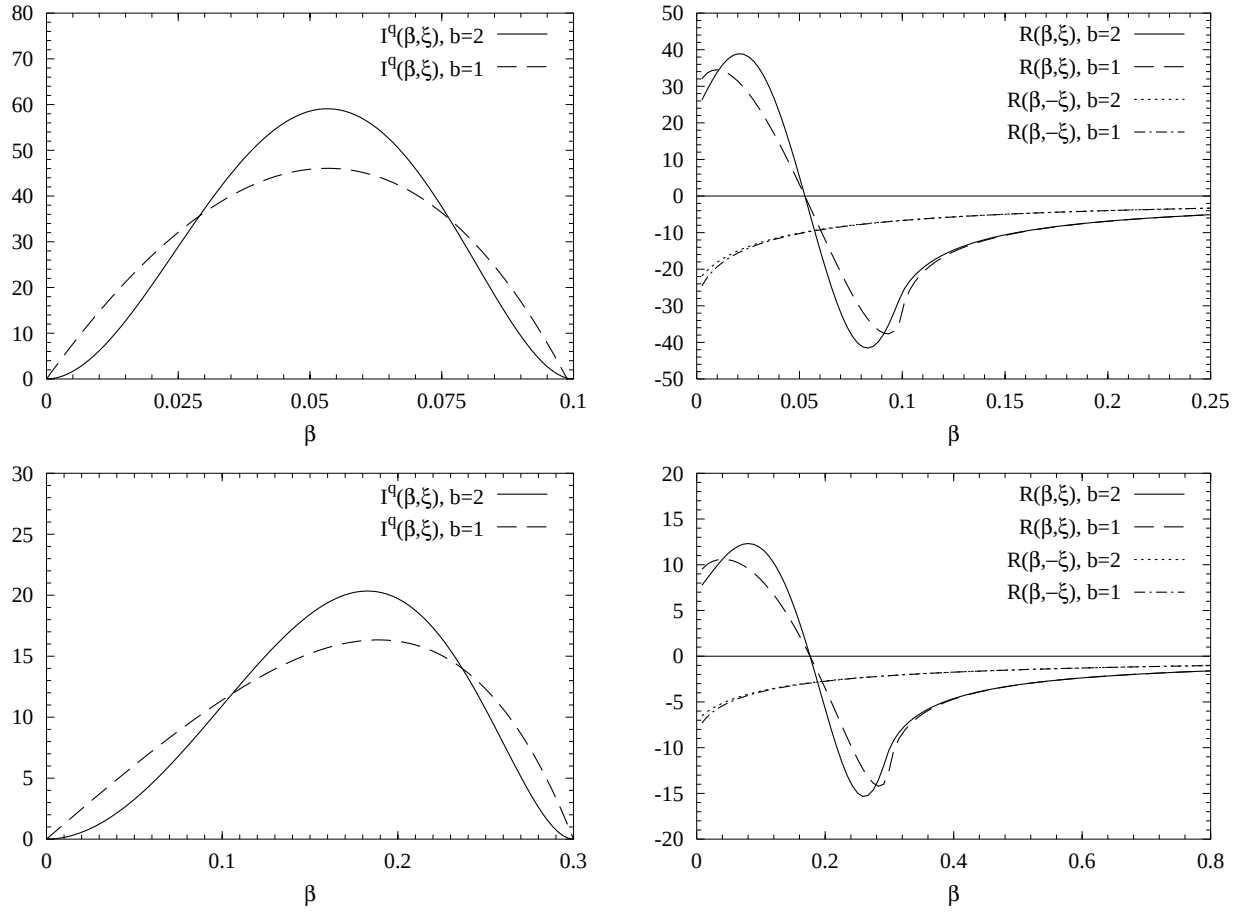

Figure 17: The functions appearing in the integrals (36) and (37) for the meson production amplitude for $\xi = 0.053$ (top) and $\xi = 0.18$ (bottom), which respectively correspond to $x_B = 0.1$ and $x_B = 0.3$. Note the different ranges for β in the plots.

form as $I^q(\xi)$ by rewriting

$$I^g(\xi) = \int_{-1}^{1} dx\, \frac{H^g(x,\xi)}{x}\, \frac{1}{\xi - x - i\epsilon} = \frac{1}{\xi} \int_{-1}^{1} dx\, \frac{H^g(x,\xi)}{\xi - x - i\epsilon}\,, \tag{35}$$

where we used that $H^g(x,\xi)$ is even in x. The imaginary parts of these integrals are readily converted into integrals over β, with

$$\begin{aligned} \mathrm{Im}\, I^q(\xi) &= \int_0^{\frac{2\xi}{1+\xi}} d\beta\, I(\beta,\xi)\, q(\beta), \\ I(\beta,\xi) &= \frac{\pi\Gamma(2b+2)}{2^{2b+1}\Gamma^2(b+1)}\, \frac{(1-\xi^2)^b}{\xi^{2b+1}}\, \frac{1}{(1-\beta)^{2b+1}} \Big(\frac{2\xi}{1+\xi} - \beta\Big)^b\, \beta^b \end{aligned} \tag{36}$$

for $\xi > 0$. The function $I(\beta,\xi)$ vanishes at the endpoints of the integration region, which in particular ensures the convergence of the integral at $\beta = 0$ for common parameterizations of quark densities. To obtain the analogous expressions for $I^{\bar q}$, $\tilde I^q$, $\tilde I^{\bar q}$ and I^g one has to replace $q(\beta)$ with $\bar q(\beta)$, $\Delta q(\beta)$, $\Delta\bar q(\beta)$ and $\beta g(\beta)$, respectively.

The real parts of the amplitudes involve principal value integrals, whose numerical evaluation requires some care, especially for small ξ. For our choices of profile parameters $b = 1$ and $b = 2$ one

can explicitly perform the α integral after inserting (32) into (34) and (35). The result is

$$\begin{aligned}
\mathrm{Re}\, I^q(\xi) &= \int_0^1 d\beta \Big[R(\beta,\xi)\, q(\beta) + R(\beta,-\xi)\, \bar{q}(\beta) \Big] \\
&= \int_0^1 d\beta \left\{ R(\beta,\xi) \Big[q(\beta) - \bar{q}(\beta) \Big] + \Big[R(\beta,\xi) + R(\beta,-\xi) \Big]\, \bar{q}(\beta) \right\}, \\
\mathrm{Re}\, I^g(\xi) &= \int_0^1 d\beta \Big[R(\beta,\xi) + R(\beta,-\xi) \Big] \beta g(\beta)\,, \\
\mathrm{Re}\, \tilde{I}^q(\xi) &= \int_0^1 d\beta \Big[R(\beta,\xi)\, \Delta q(\beta) - R(\beta,-\xi)\, \Delta\bar{q}(\beta) \Big]\,, \qquad (37)
\end{aligned}$$

with

$$\begin{aligned}
R(\beta,\xi) &\overset{b=1}{=} -\frac{3}{4\xi^3(1-\beta)^3} \left(2\xi(1-\beta)(\beta-\xi) \right. \\
&\qquad \left. + \beta(1-\xi) \Big[\beta(1+\xi) - 2\xi \Big] \log \frac{|\beta(1+\xi)-2\xi|}{\beta(1-\xi)} \right), \\
R(\beta,\xi) &\overset{b=2}{=} \frac{5}{16\xi^5(1-\beta)^5} \left(2\xi(1-\beta)(\beta-\xi) \Big[3(\beta-\xi)^2 - 5\xi^2(1-\beta)^2 \Big] \right. \\
&\qquad \left. + 3\beta^2(1-\xi)^2 \Big[\beta(1+\xi) - 2\xi \Big]^2 \log \frac{|\beta(1+\xi)-2\xi|}{\beta(1-\xi)} \right). \qquad (38)
\end{aligned}$$

For both $b = 1$ and $b = 2$, the function $R(\beta,\xi)$ is continuous in the full interval of integration, with finite limits at $\beta = 0$ and $\beta = 1$. If $\xi > 0$ it is positive for $\beta < \xi$ and negative for $\beta > \xi$, and if $\xi < 0$ it is negative in the entire interval. Convergence of the integral for polarized quark distributions requires that $\Delta q(\beta)$ and $\Delta\bar{q}(\beta)$ have integrable singularities at $\beta = 0$, which is the case for the parton densities we use in this study. The unpolarized quark distributions have a steeper behavior at small β, but since $R(\beta,\xi) + R(\beta,-\xi) \sim \beta$ for $\beta \to 0$ it is sufficient to have integrable singularities for $q(\beta) - \bar{q}(\beta)$ and for $\beta\bar{q}(\beta)$.

In Fig. 17 we illustrate the behavior of the functions multiplying the parton distributions in the integrals (36) and (37). The imaginary part of the amplitude involves momentum fractions in the parton densities between 0 and $2\xi/(1+\xi) = x_B$, with a maximum of the shape function $I(\beta,\xi)$ for β around ξ. In contrast, the real part is sensitive to higher momentum fractions, with a partial cancellation from values above and below ξ. One also clearly sees the stronger sensitivity to small β if $b = 1$. Note that the functions shown in the figure will be multiplied in the amplitude with functions showing a strong rise towards $\beta = 0$.

B Distribution of pions or kaons from vector meson decay

In this appendix we discuss the decay of a vector meson into two pseudoscalar mesons and derive the z distribution given in (27). Consider the contribution of $ep \to VB$ with subsequent decay $V \to P_1 P_2$ to semi-inclusive production $ep \to P_1 + X$. A useful set of variables to describe the decay of the vector meson are the polar and azimuthal angles θ and φ of P_1 in the vector meson center-of-mass, as shown in Fig. 18. The distribution in these angles is connected in a straightforward way with the spin density matrix of the produced vector meson [57], and the phase space element has a factorized form in the variables Q^2, x_B, t and θ, φ. The variable z used for semi-inclusive production of P_1 is then given by

$$z = a + b\cos\theta + c\sin\theta\cos\varphi \qquad (39)$$

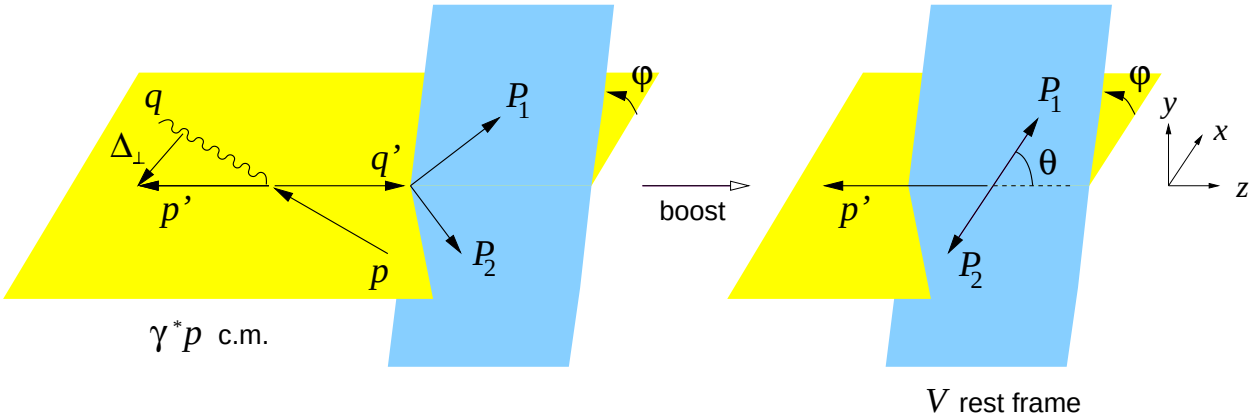

Figure 18: Kinematic variables for $\gamma^*(q) + p(p) \to V(q') + B(p')$ followed by the decay $V \to P_1 P_2$, shown in the $\gamma^* p$ center-of-mass and in the rest frame of V. Here θ and φ are the spherical coordinates of the momentum of P_1 in the depicted coordinate system.

with

$$\begin{aligned}
a &= \frac{E_{P1}}{m_V}\,\frac{r_2\,(1+2x_B\,m_p^2/Q^2)+r_3\sqrt{1+4x_B^2\,m_p^2/Q^2}}{2r_1}\,\Big[1+O(x_B\Delta_T^2/Q^2)\Big] \;\approx\; \frac{E_{P1}}{m_V}\,,\\
b &= \frac{|\boldsymbol{q}_{P1}|}{m_V}\,\frac{r_3\,(1+2x_B\,m_p^2/Q^2)+r_2\sqrt{1+4x_B^2\,m_p^2/Q^2}}{2r_1}\,\Big[1+O(x_B\Delta_T^2/Q^2)\Big] \;\approx\; \frac{|\boldsymbol{q}_{P1}|}{m_V}\,,\\
c &= -\,\frac{|\boldsymbol{q}_{P1}|\Delta_T}{Q^2}\,\frac{2x_B}{1-x_B}\,\frac{\sqrt{1+4x_B^2\,m_p^2/Q^2}}{r_3}\,,
\end{aligned} \tag{40}$$

where we abbreviated

$$\begin{aligned}
r_1 &= 1+\frac{x_B}{1-x_B}\,\frac{m_p^2}{Q^2}\,, \qquad\qquad r_2 \;=\; 1+\frac{x_B}{1-x_B}\,\frac{m_V^2-m_B^2+m_p^2}{Q^2}\,,\\
r_3 &= \left[\left(1-\frac{x_B}{1-x_B}\,\frac{m_V^2+m_B^2-m_p^2}{Q^2}\right)^2-\left(\frac{x_B}{1-x_B}\,\frac{2m_V m_B}{Q^2}\right)^2\right]^{1/2}.
\end{aligned} \tag{41}$$

The energy and momentum E_{P1} and $|\boldsymbol{q}_{P1}|$ of P_1 in the rest frame of V have already been given in (30), and Δ_T is the transverse momentum of the scattered baryon with respect to the initial proton in the $\gamma^* p$ center-of-mass (see Fig. 18). The approximate expressions in (40) are valid up to relative corrections of order $x_B\,m_p^2/Q^2$ and $x_B\,\Delta_T^2/Q^2$, and to the same accuracy one has $\Delta_T^2 = (1-x_B)(t_0-t)$. Changing variables from θ to z gives for the cross section

$$\frac{d\sigma(ep\to P_1+P_2\,B)}{dQ^2\,dx_B\,dt\,d\varphi\,dz} = \frac{1}{b-c\cot\theta\cos\varphi}\,\frac{d\sigma(ep\to P_1+P_2\,B)}{dQ^2\,dx_B\,dt\,d\varphi\,d\cos\theta}. \tag{42}$$

In Bjorken kinematics one has $c \ll b$ and can replace the Jacobian in (42) by $1/b$ (except in the small region where $\sin\theta \sim c/b$, which is not relevant for our purposes). Neglecting Δ_T we get $z = a + b\cos\theta$ with a and b evaluated at $\Delta_T = 0$, and integration over t and φ gives

$$\frac{d\sigma(ep\to P_1+P_2\,B)}{dQ^2\,dx_B\,dz} = \frac{3}{4b^3}\left[2(z-a)^2\,\frac{d\sigma(ep\to V_L\,B)}{dQ^2\,dx_B}+(z-a+b)(a+b-z)\frac{d\sigma(ep\to V_T\,B)}{dQ^2\,dx_B}\right] \tag{43}$$

in terms of the cross sections for the production of longitudinally or transversely polarized vector mesons. Using s-channel helicity conservation, which is experimentally seen to hold at the few 10% level in ρ^0 and ϕ production [11, 12, 13], these cross sections respectively correspond to the production from longitudinally or transversely polarized virtual photons, and we finally obtain (27). In our numerical applications we have used the exact expressions from (40) and (41) at $\Delta_T = 0$, and thus in particular neglected c. Since the integrated cross sections are dominated by small Δ_T, this should be a very good approximation for the values of Q^2 and x_B we focus on in the present study. The inclusion of finite Δ_T effects in the kinematics would considerably complicate any analysis.

References

[1] A. Airapetian *et al.* [HERMES Collaboration], Phys. Rev. D **71**, 012003 (2005) [hep-ex/0407032].

[2] A. Airapetian *et al.* [HERMES Collaboration], Phys. Rev. Lett. **94**, 012002 (2005) [hep-ex/0408013].

[3] X. D. Ji, J. Phys. G **24**, 1181 (1998) [hep-ph/9807358].

[4] K. Goeke, M. V. Polyakov and M. Vanderhaeghen, Prog. Part. Nucl. Phys. **47**, 401 (2001) [hep-ph/0106012].

[5] M. Burkardt, Int. J. Mod. Phys. A **18**, 173 (2003) [hep-ph/0207047].

[6] M. Diehl, Phys. Rept. **388**, 41 (2003) [hep-ph/0307382].

[7] A. V. Belitsky and A. V. Radyushkin, hep-ph/0504030.

[8] A. Szczurek, V. Uleshchenko and J. Speth, Phys. Rev. D **63**, 114005 (2001) [hep-ph/0009318]; V. Uleshchenko and A. Szczurek, Acta Phys. Polon. B **33**, 3299 (2002) [hep-ph/0207049].

[9] B. Maiheu, talk given at the 13th International Workshop on Deep Inelastic Scattering (DIS 05), Madison, WI, USA, May 2005, to appear in the Proceedings.

[10] A. Airapetian *et al.* [HERMES Collaboration], Eur. Phys. J. C **17**, 389 (2000) [hep-ex/0004023].

[11] A. B. Borissov [HERMES Collaboration], Nucl. Phys. Proc. Suppl. **99A**, 156 (2001);
A. B. Borissov [HERMES Collaboration], Procs. of the 9th International Workshop on High-Energy Spin Physics (SPIN 01), Dubna, Russia, Aug. 2001, DESY-HERMES-01-60.

[12] M. Tytgat, Doctoral thesis, Universiteit Gent, 2000.

[13] G. L. Rakness, Doctoral thesis, University of Colorado at Boulder, 2000.

[14] C. Hadjidakis *et al.* [CLAS Collaboration], Phys. Lett. B **605**, 256 (2005) [hep-ex/0408005].

[15] J. C. Collins, L. Frankfurt and M. Strikman, Phys. Rev. D **56**, 2982 (1997) [hep-ph/9611433].

[16] L. N. Hand, Phys. Rev. **129**, 1834 (1963).

[17] M. Diehl, B. Pire and L. Szymanowski, Phys. Lett. B **584**, 58 (2004) [hep-ph/0312125].

[18] M. Beneke and M. Neubert, Nucl. Phys. B **675**, 333 (2003) [hep-ph/0308039].

[19] I. V. Anikin, B. Pire, L. Szymanowski, O. V. Teryaev and S. Wallon, hep-ph/0411408.

[20] I. V. Musatov and A. V. Radyushkin, Phys. Rev. D **61**, 074027 (2000) [hep-ph/9905376].

[21] M. Diehl, T. Feldmann, R. Jakob and P. Kroll, Eur. Phys. J. C **39**, 1 (2005) [hep-ph/0408173].

[22] L. Frankfurt, M. Strikman and C. Weiss, Phys. Rev. D **69**, 114010 (2004) [hep-ph/0311231].

[23] Ph. Hägler *et al.* [LHPC Collaboration], Phys. Rev. Lett. **93**, 112001 (2004) [hep-lat/0312014].

[24] C. Adloff *et al.* [H1 Collaboration], Eur. Phys. J. C **13**, 371 (2000) [hep-ex/9902019].

[25] M. Diehl and A. V. Vinnikov, Phys. Lett. B **609** (2005) 286 [hep-ph/0412162].

[26] L. L. Frankfurt, M. V. Polyakov, M. Strikman and M. Vanderhaeghen, Phys. Rev. Lett. **84**, 2589 (2000) [hep-ph/9911381].

[27] L. Mankiewicz, G. Piller and A. Radyushkin, Eur. Phys. J. C **10**, 307 (1999) [hep-ph/9812467].

[28] M. Penttinen, M. V. Polyakov and K. Goeke, Phys. Rev. D **62**, 014024 (2000) [hep-ph/9909489].

[29] W. Koepf, L. L. Frankfurt and M. Strikman, Phys. Rev. D **53**, 2586 (1996) [hep-ph/9507218].

[30] M. Diehl, P. Kroll and C. Vogt, Eur. Phys. J. C **22**, 439 (2001) [hep-ph/0108220].

[31] A. P. Bakulev, S. V. Mikhailov and N. G. Stefanis, Phys. Lett. B **578**, 91 (2004) [hep-ph/0303039].

[32] A. Khodjamirian, T. Mannel and M. Melcher, Phys. Rev. D **70**, 094002 (2004) [hep-ph/0407226].

[33] V. M. Braun and A. Lenz, Phys. Rev. D **70**, 074020 (2004) [hep-ph/0407282].

[34] E. Leader, A. V. Sidorov and D. B. Stamenov, Phys. Rev. D **58**, 114028 (1998) [hep-ph/9807251].

[35] J. Blümlein and H. Böttcher, Nucl. Phys. B **636**, 225 (2002) [hep-ph/0203155].

[36] T. Feldmann, Int. J. Mod. Phys. A **15**, 159 (2000) [hep-ph/9907491].

[37] J. Pumplin, D. R. Stump, J. Huston, H. L. Lai, P. Nadolsky and W. K. Tung, JHEP **0207**, 012 (2002) [hep-ph/0201195].

[38] A. D. Martin, R. G. Roberts, W. J. Stirling and R. S. Thorne, Phys. Lett. B **531**, 216 (2002) [hep-ph/0201127].

[39] A. D. Martin, R. G. Roberts, W. J. Stirling and R. S. Thorne, Eur. Phys. J. C **28**, 455 (2003) [hep-ph/0211080]; Phys. Lett. B **604**, 61 (2004) [hep-ph/0410230].

[40] S. Alekhin, Phys. Rev. D **68**, 014002 (2003) [hep-ph/0211096].

[41] D. Y. Ivanov, L. Szymanowski and G. Krasnikov, JETP Lett. **80**, 226 (2004) [hep-ph/0407207].

[42] B. Lehmann-Dronke, P. V. Pobylitsa, M. V. Polyakov, A. Schäfer and K. Goeke, Phys. Lett. B **475**, 147 (2000) [hep-ph/9910310].

[43] M. V. Polyakov and C. Weiss, Phys. Rev. D **60**, 114017 (1999) [hep-ph/9902451].

[44] N. Kivel, M. V. Polyakov and M. Vanderhaeghen, Phys. Rev. D **63**, 114014 (2001) [hep-ph/0012136].

[45] P. Schweitzer, S. Boffi and M. Radici, Phys. Rev. D **66**, 114004 (2002) [hep-ph/0207230].

[46] L. Frankfurt, W. Koepf and M. Strikman, Phys. Rev. D **54**, 3194 (1996) [hep-ph/9509311]; Phys. Rev. D **57**, 512 (1998) [hep-ph/9702216].

[47] M. Vanderhaeghen, P. A. M. Guichon and M. Guidal, Phys. Rev. D **60**, 094017 (1999) [hep-ph/9905372].

[48] S. V. Goloskokov and P. Kroll, hep-ph/0501242.

[49] A. B. Borissov, private communication.

[50] K. Lukashin *et al.* [CLAS Collaboration], Phys. Rev. C **63**, 065205 (2001) [hep-ex/0101030].

[51] L. Morand [CLAS Collaboration], hep-ex/0504057.

[52] J. Volmer *et al.* [The Jefferson Lab F_π Collaboration], Phys. Rev. Lett. **86**, 1713 (2001) [nucl-ex/0010009].

[53] C. J. Bebek *et al.*, Phys. Rev. D **17**, 1693 (1978).

[54] R. Jakob, P. Kroll and M. Raulfs, J. Phys. G **22**, 45 (1996) [hep-ph/9410304];
V. M. Braun, A. Khodjamirian and M. Maul, Phys. Rev. D **61**, 073004 (2000) [hep-ph/9907495];
A. P. Bakulev, A. V. Radyushkin and N. G. Stefanis, Phys. Rev. D **62**, 113001 (2000) [hep-ph/0005085];
N. G. Stefanis, W. Schroers and H. C. Kim, Eur. Phys. J. C **18**, 137 (2000) [hep-ph/0005218].

[55] C. Hadjidakis, D. Hasch and E. Thomas [HERMES Collaboration], Int. J. Mod. Phys. A **20**, 593 (2005) [hep-ex/0405078].

[56] C. Hadjidakis, private communication.

[57] K. Schilling and G. Wolf, Nucl. Phys. B **61**, 381 (1973).

[58] S. Kretzer, Phys. Rev. D **62**, 054001 (2000) [hep-ph/0003177].